ENGINEERING PROPERTIES OF VEGETATION
2

M.E.Styczen and R.P.C.Morgan

2.1 INTRODUCTION

Vegetation provides a protective layer or buffer between the atmosphere and the soil. Through the hydrological cycle, it affects the transfer of water from the atmosphere to the earth's surface, soil and underlying rock. It therefore influences the volume of water contained in rivers, lakes, the soil and groundwater reserves. The above-ground components of the vegetation, such as leaves and stems, partially absorb the energy of the erosive agents of water and wind, so that less is directed at the soil, whilst the below-ground components, comprising the rooting system, contribute to the mechanical strength of the soil.

Traditionally, the role of vegetation has been viewed rather simplistically, as seen by the somewhat superficial way it is dealt with in water erosion studies. The most commonly used approach has been to assign to it a coefficient, such as the C-factor in the Universal Soil Loss Equation (Wischmeier and Smith, 1978) which, for a certain stage of growth and plant density, describes the ratio of soil loss when vegetation is present to the amount lost on a bare soil. Values of this soil loss ratio are derived experimentally from field trials and, while they are true values for those situations, they cannot be readily used to predict the effect of the same or other vegetation in different climatic and pedological conditions.

Wischmeier (1975) tried to split the C-factor into C_I, C_{II} and C_{III} subfactors (Figure 2.1). C_I describes the effect of the presence of a plant canopy at some elevation above the soil. C_{II} is defined as the effect of a mulch or close-growing vegetation in direct contact with the soil surface. Root effects are not included. C_{III} represents the residual effects of land use on soil structure, organic matter content and soil density, the effects of tillage or lack of tillage on surface roughness and soil porosity, and the effects of roots, subsurface stems and biological activity in the soil. This approach has been used in erosion prediction models (Beasley, Huggins and Monke, 1980; Park, 1981; Park, Mitchell and Scarborough, 1982) but is limiting because at least two of the three subfactors may influence more than one erosion process. It is difficult therefore to give them a precise physical meaning.

The conflicting views, provided by field and laboratory experiments (Figure 2.2) on what level of vegetation cover is required to reduce the soil loss ratio from 1.0 to 0.5, illustrate the inadequacy of the above approach. In order to understand the role of vegetation in combating erosion it is necessary to:

1. understand the erosion processes;
2. consider how each of these processes may be affected by vegetation;
3. determine the salient properties of the vegetation which most affect these processes;
4. try to quantify the combined effect of vegetation on the processes acting together in different situations.

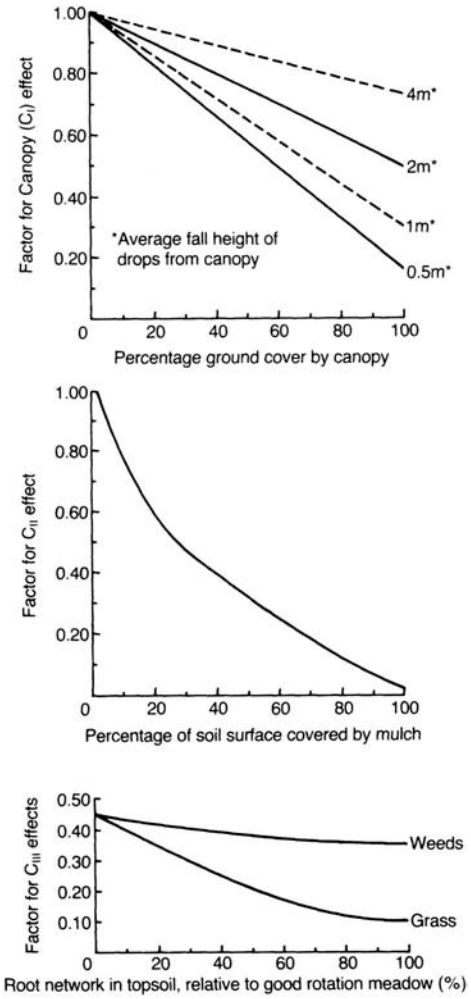

Figure 2.1 Soil loss ratios for subfactors of the C-factor in the Universal Soil Loss Equation (after Wischmeier, 1975). C_I describes the canopy effect, C_{II} the effect of plant residues and ground vegetation, and C_{III} the residual effects of previous land use. The graph shown here for the C_{III} effect applies to previously undisturbed land only and not to cropland or construction sites.

Such a detailed understanding is difficult to achieve. It is hampered by the fact that much previous research has concentrated on establishing C-factor values rather than on understanding how vegetation operates within the erosion system. Analysis is also hampered by the complexity of the interaction between vegetation, climate, soil properties and hydrology. Nevertheless, the relatively low rates of erosion observed

Slope Stabilization and Erosion Control: A Bioengineering Approach. Edited by R.P.C.Morgan and R.J.Rickson. Published in 1995 by E & FN Spon, 2–6 Boundary Row, London, SE1 8HN. ISBN 0 419 15630 5.

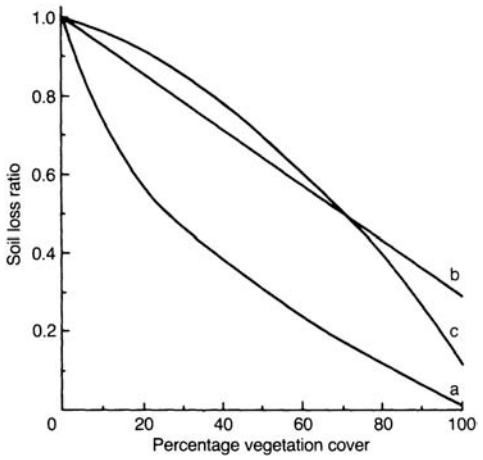

Figure 2.2 Examples of relationships between the soil loss ratio and percentage vegetation cover. a=ground level vegetation (Laflen and Colvin, 1981); b=vegetation canopy at 1 m above the ground (Wischmeier, 1975); c=oat straw mulch (Singer and Blackard, 1978).

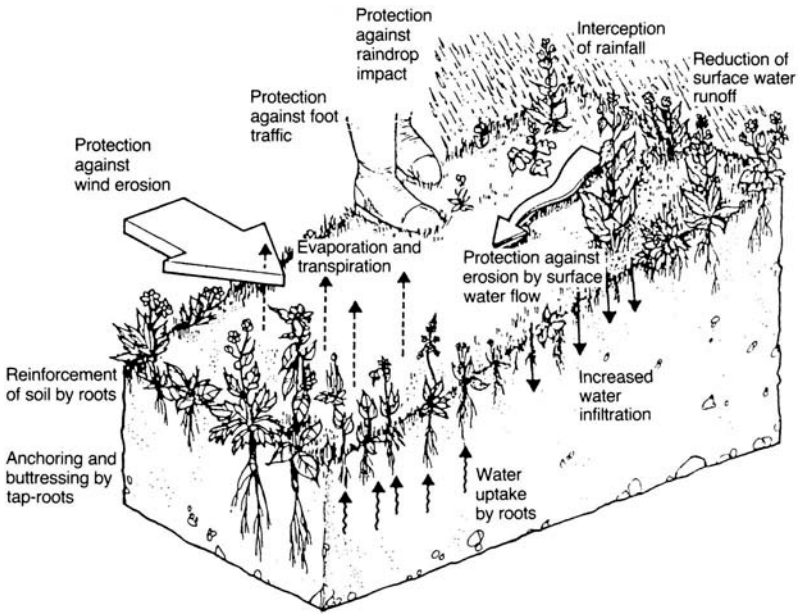
Protection against raindrop impact
Interception of rainfall
Reduction of surface water runoff
Protection against foot traffic
Protection against wind erosion
Evaporation and transpiration
Protection against erosion by surface water flow
Reinforcement of soil by roots
Increased water infiltration
Anchoring and buttressing by tap-roots
Water uptake by roots

Figure 2.3 Engineering role of vegetation (after Coppin and Richards, 1990).

in well-vegetated areas compared with the catastrophic rates which can arise when vegetation is cleared, demonstrate that vegetation performs a major engineering role in protecting the landscape. This chapter aims to explore that role by reviewing its hydrological, hydraulic and mechanical effects. These are summarized diagrammatically in Figure 2.3.

2.2
HYDROLOGICAL EFFECTS OF VEGETATION

2.2.1
EVAPOTRANSPIRATION

Evapotranspiration is the combined process of the removal of moisture from the earth's surtace by evaporation and transpiration from the vegetation cover. Evapotranspiration from plant surfaces is compared to the equivalent evaporation from an open water body. The two rates are not the same because the energy balances of the surfaces are markedly different. For example, the albedo value, defined as the proportion of incoming short-wave radiation which is reflected, is, depending on the altitude of the sun, about 0.1 for water, but varies between 0.1 and 0.3 for a plant cover. The effect of vegetation is expressed by the E_t/E_o ratio, where E_t is the evapotranspiration rate for the vegetation cover and E_o is the evaporation rate for open water. Table 2.1 gives some typical values for plant covers at different stages of growth and in different seasons (Withers and Vipond, 1974; Doorenbos and Pruitt, 1977).

The values of E_t/E_o ratios assume that evapotranspiration is not limited by the supply of water; in other words, it is taking place at the potential rate (E_p). Where high rates of evapotranspiration occur, however, the top layers of the soil rapidly dry out and the plants find it more difficult to extract water from the soil by suction through the roots. To prevent dehydration, plants reduce their transpiration so that actual evapotranspiration (E_a) becomes less than potential. The ratio of actual to potential evapotranspiration (E_a/E_p) depends upon the soil moisture deficit (SMD) which is defined as the difference between the reduced soil moisture level and that pertaining at field capacity. The

Table 2.1 E_t/E_o ratios for selected plant covers (after Withers and Vipond, 1974; Doorenbos and Pruitt, 1977)

Plant (crop) cover	E_t/E_o *ratio*
Wet (padi) rice	1.35
Wheat	0.59–0.61
Maize	0.67–0.70
Barley	0.56–0.60
Millet/sorghum	0.62
Potato	0.70–0.80
Beans	0.62–0.69
Groundnut	0.50–0.87
Cabbage/Brussels sprouts	0.45–0.70
Banana	0.70–0.77
Tea	0.85–1.00
Coffee	0.50–1.00
Cocoa	1.00
Sugar cane	0.68–0.80
Sugar beet	0.73–0.75
Rubber	0.90
Oil palm	1.20
Cotton	0.63–0.69

Plant (crop) cover	E_t/E_o *ratio*
Cultivated grass	0.85–0.87
Prairie/savanna grass	0.80–0.95
Forest/woodland	0.90–1.00

amount of soil moisture which can be extracted by a plant cover when water is not limiting is defined by a root constant *(C);* typical values are given in Table 2.2 (Grindley, 1969). Actual evapotranspiration taking place as a soil dries out can be estimated using the model of Penman (1949) whereby actual evapotranspiration equals potential $(E_a=E_p)$ as long as SMD<C but when SMD>C, a further 25 mm of moisture can be extracted at a reduced rate until, at SMD>3C, extraction becomes minimal ($E_a=0.1E_p$).

Although the ability of vegetation to reduce soil moisture is recognized qualitatively, it is hard to quantify. Reduced soil moisture increases soil suction which affects both hydraulic conductivity and pore-water pressure. Only limited information is available, however, on differences in the hydraulic conductivity of soils with and without a vegetation cover and the effect of vegetation on slope stability through soil moisture depletion is difficult to separate from that of soil reinforcement by the rooting system. Nevertheless, through modification of the soil moisture content, vegetation affects the frequency at which the soil becomes saturated which, in turn, controls the likelihood of runoff generation or mass soil failure. The strength of this effect depends upon the local soil and climatic conditions and the vegetation type. It will also show, often substantial, seasonal variation, being greatest in summer and lowest in winter or whenever the vegetation is dormant.

2.2.2 INTERCEPTION

On contact with the canopy of a vegetation cover, the rainfall is divided into two parts. These are (1) direct throughfall, that which reaches the ground after passing through gaps in the canopy, and (2) interception, that which strikes the vegetation cover. If it is assumed that

Table 2.2 Values of the root constant *(C)* for use in estimating evapotranspiration (after Grindley, 1969)

Vegetation	*Maximum SMD (mm)*[a]	*Root constant, C (mm)*
Cereals	200	140
Temporary grass	100	56
Permanent grass	125	75
Rough grazing	50	13
Trees (mature stand)	125–250	75–200

[a] SMD=soil moisture deficit. The actual value of maximum SMD varies with the depth of roots, being higher for deep-rooted vegetation than for shallow-rooted types.

the rain falls vertically, the volume of rainfall intercepted *(IC)* can be calculated from the simple relationship:

$$IC = \text{RAIN} \cdot CC, \tag{2.1}$$

where CC=percentage canopy cover.

Some of the intercepted rainfall is stored on the leaves and stems and is later returned to the atmosphere by evaporation. The remainder of the intercepted rainfall, termed 'temporarily intercepted throughfall' (TIF), reaches the ground either as stemflow (i.e. that running down the stems, branches or trunks of the vegetation) or as leaf drainage.

Interception storage

Observed interception storage (IC_{store}) varies widely, depending upon the type of vegetation and the intensity of the rain, but, during a storm, it increases exponentially to a maximum value (IC_{max}) in a relationship similar to that proposed by Merriam (1973):

$$IC_{store} = IC_{max}(1 - \exp R_{cum}/IC_{max}), \tag{2.2}$$

where R_{cum} is the cumulative rainfall received since the start of the storm. Values of maximum interception storage are difficult to determine but probably range from 0.5 mm for deciduous forest in winter to 1 mm for coniferous forest, deciduous forest in summer and many agricultural crops, 1–2 mm for grasses and 2.5 mm for a multi-layered tropical rain forest (Table 2.3). Since storage often returns to the maximum value between storms, its cumulative effect over a year can be considerable and can account for 10–15% of the annual rainfall in cool-temperate hardwood forests, 15–25% in temperate broad-leaved forests, 20–25% for cereals and grass covers, and 25–30% in temperate coniferous and in tropical rain forests. Interception storage thus reduces the volume of rainfall reaching the ground surface by these amounts.

Stemflow

The amount of water shed by stemflow depends upon the angle of the stems of the plant to the ground surface (De Ploey, 1982; van Elewijck, 1989). For plants where the stem diameters are less than the median volume drop size of the rainfall, such as grasses, stemflow is at a maximum when the stem angles are between 50° and 70°. For plants with larger diameter stems, the situation is less clear. Van Elewijck (1988) recorded maximum stemflow on maize leaves at stem angles between 10° and 20° and on simulated branches at stem angles between 5° and 15° whereas Herwitz (1987) found that stemflow on branches (>4cm diameter) of *Toona australis* and *Aleurites moluccana* increased linearly with stem angle to reach a maximum at a branch angle of 60°, the highest angle used in his experiments.

Very little information exists on volumes of stemflow. Measurements by Noble (1981) and Finney (1984) show stemflow volumes to be about 3–7% of storm rainfall for both Brussels sprouts with canopy covers of 40–50% and potatoes with 20–25% canopy. Higher values were observed for sugar beet at 42% of storm rainfall with 28% canopy cover (Finney, 1984). A figure of 55% was also recorded for sugar beet by Appelmans, van Hove and De Leenheer (1980). Values of 44% and 31% were recorded by Bui and Box (1992) in laboratory experiments under maize and sorghum respectively. High stemflow volumes can therefore be expected for plants with an architecture designed to concentrate water at their base and characterized by stems and leaves which converge towards the ground. De Ploey (1982) estimates that tussocky grasses may produce stemflow volumes that amount to 50–100% of the intercepted rainfall and Herwitz (1987) found that more than 80% of the impacting rain on tree branches inclined at 60° contributed to stemflow. Such concentrations of rainfall over relatively small areas can increase the effective rainfall intensity locally beneath tussocky grasses to 150–200% of that received at the top of the canopy (De Ploey, 1982). Even greater concentrations can occur in forests. Herwitz (1986) recorded an instance in the tropical rain forest in northern Queensland where stemflow fluxes measured during a rain

Table 2.3 Interception storage capacity for different vegetation types (after Horton, 1919; Leyton, Reynolds and Thompson, 1967; Zinke, 1967; Rutter and Morton, 1977; Herwitz, 1985)

Vegetation type	*Interception storage capacity, IC_{max}(mm)*
Fescue grass	1.2
Molinia	0.2
Rye grass	2.5
Meadow grass, clover	2.0
Blue stem grass	2.3
Heather	1.5
Bracken	1.3
Tropical rain forest	0.8–2.5
Temperate deciduous forest (summer)	1.0
Temperate deciduous forest (winter)	0.5
Needle leaf forest (pines)	1.0
Needle leaf forest (spruce, firs)	1.5
Evergreen hardwood forest	0.8
Soya beans	0.7
Potatoes	0.9
Cabbage	0.5
Brussels sprouts	1.0
Sugar beet	0.6
Millet	0.3
Spring wheat	1.8
Winter wheat	3.0
Barley, rye, oats	1.2
Maize	0.8
Tobacco	1.8
Alfalfa	2.8
Apple	0.5

fall of 11.8 mm in 6 min gave local depth equivalents of between 83 and 1888 mm. These large quantities of water beneath plants can play an important role in the generation of runoff.

Based on the work of van Elewijck (1988), the volume of stemflow (SF) may be estimated as a function of the average angle of the plant stems to the ground (PA) using the following equations:

for stem diameters<median volume drop diameter:

$$SF = TIF\ (\cos PA \cdot \sin^2 PA); \tag{2.3}$$

for stem diameters>median volume drop diameter:

$$SF = TIF \cos PA. \tag{2.4}$$

In the above, sin PA expresses the effect of gravity and cos PA expresses the effect of the projected length of the leaves and stems on the plant.

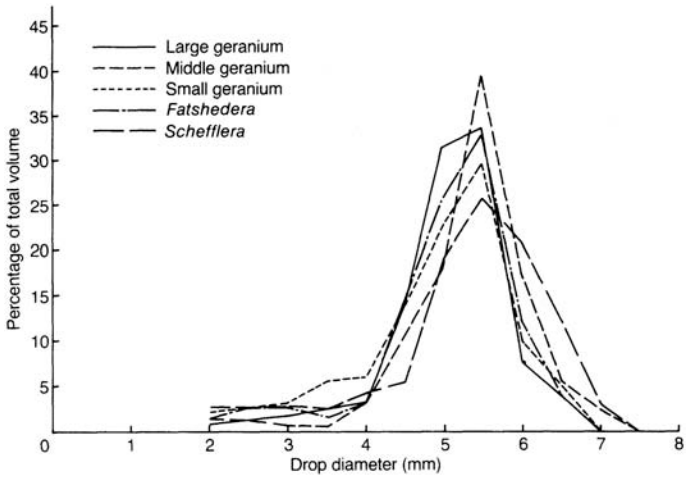

Figure 2.4 Drop-size distribution of leaf drainage (after Brandt, 1989).

Leaf drainage

The volume of leaf drainage is equal to the volume of temporarily intercepted throughfall less the volume of stemflow. Leaf drainage comprises raindrops that are shattered into small droplets immediately they strike the vegetation and large drops formed by the temporary storage and coalescence of raindrops on the leaf and stem surfaces before they fall to the ground. Thus the rainfall beneath a plant canopy has higher proportions of small (<1 mm) and large (>5 mm) drops and fewer medium-sized drops compared with the original rainfall. In this way the canopy cover changes the drop-size distribution of the rain.

For plants with long leaves, like maize, the drops are mainly channelled along the centre vein and form leaf drips with diameters of 5–5.5 mm. For soya beans, the average size of the leaf drips is smaller, at about 4.5 mm, partly because more raindrops are rejected instantaneously by the leaves (Armstrong and Mitchell, 1987). Brandt (1989), in a review of previous literature combined with results of her own laboratory studies, concludes that leaf drainage has a normal drop-size distribution with a mean volume drop diameter of between 4.52 and 4.95 mm and a standard deviation of 0.79– 1.30 mm (Figure 2.4).

Concentrations of water from leaf drip points can result in very high localized rainfall intensities, over 1000% greater than the intensity received at the canopy (Armstrong and Mitchell, 1987). These can exceed infiltration rates and result in surface runoff. This effect would be most marked in calm conditions. In strong winds, movement of the leaves and branches, as well as the falling water drops, will help to spread the leaf drainage more uniformly.

Soil detachment by raindrop impact

Soil detachment by raindrop impact has been related to various properties of the rain; KE (kinetic energy), EI_{30} (kinetic energy times the maximum intensity of the storm, measured over 30 min) and I^2 (intensity squared) being the most commonly used parameters. Vegetation affects these properties by altering the mass of rainfall reaching the ground, its drop-size distribution and its local intensity.

The energy of the rainfall available for soil detachment under a vegetation cover is dependent upon the relative proportions of the rain falling as direct throughfall and as leaf drainage. The ability of stemflow to detach soil particles is normally ignored. Thus the kinetic energy of the rain can be expressed by the simple arithmetical relationship:

$$KE = [(DT/TV) \cdot KE(DT)] + [(LD/TV) \cdot KE(LD)], \quad (2.5)$$

where KE=the kinetic energy (J/m^2 mm) of the rain; DT=the volume of direct throughfall; LD=the volume of leaf drainage; and TV=the total volume of direct throughfall and leaf drainage.

The energy of the direct throughfall is assumed to be the same as that of the natural rainfall. A reasonable approximation of the drop-size distribution of steady rain in temperate mid-latitude climates is that described by Marshall and Palmer (1948):

$$N(\delta) = N_0 e^{-\Lambda\delta}, \quad (2.6)$$

where $N(\delta)d\delta$=the number of drops per unit volume with diameters between δ and $\delta+d\delta$; $\Lambda(I)=41\ I^{-0.21}$, where Λ has units of cm^{-1} and I is the rainfall intensity (mm/h); and N_0=approximately 0.08 cm^{-4}.

Other drop-size distributions have been presented by Carter *et al.* (1974) for Florida, Hudson (1963) for Zimbabwe, and Kowal and Kassam (1976) for northern Nigeria. In the case of the Marshall-Palmer distribution, the kinetic energy (J/m^2 mm) of a unit rain can be estimated from (Brandt, 1990):

$$KE(DT) = 8.95 + 8.44 \log I, \quad (2.7)$$

where I=the intensity of the rain (mm/h).

If the drop-size distribution of the leaf drainage follows that described above, its energy may be calculated from (Brandt, 1990):

$$KE(LD) = (15.8 \cdot PH^{0.5}) - 5.87, \quad (2.8)$$

where PH=the effective height (m) of the vegetation canopy.

For non-cohesive soils, the rainfall energy is not spent on detaching individual soil particles from the soil mass. It is primarily used for deformation of the surface and the lifting and moving of the already-discrete particles. In this case, splash erosion can be expected to be proportional to the kinetic energy of the rain (Free, 1960; Moss and Green, 1987), which is approximately proportional to $I^{1.14}$. Soil detachment (DET; g/m^2), in the sense of dislodgement of soil particles by raindrop impact, can then be estimated from the simple relationship:

$$DET = k \cdot KE^{1.0} \cdot e^{-ah}, \quad (2.9)$$

where k=an index of the detachability of the soil (g/J); h=the depth (m) of the surface water layer, if any; and a=an experimental coefficient varying between 1.0 and 3.0 in value, depending upon the soil texture (Torri, Sfalanga and Del Sette, 1987).

It follows from this analysis that the rate of soil detachment beneath a vegetation cover depends upon the percentage canopy area, which controls the volumes of direct throughfall and leaf drainage, and the height of the canopy, which determines the energy of the leaf drainage. Numerous studies have shown that the energy of rain under vegetation can exceed that of an equivalent rainfall in open ground, both for trees (Chapman, 1948; Wiersum, Budirijanto and Rhomdoni, 1979; Maene and Chong, 1979; Mosley, 1982) and for lower-growing agricultural crops (Noble and Morgan, 1983; Morgan, 1985) with consequent increases in the rate of detachment (Finney, 1984; Wiersum, 1985). Field measurements with rainfall simulation showed that soil detachment under maize increased with percentage cover to double that recorded on bare soil when the canopy reached about 90% cover and was about 2m above ground level (Morgan, 1985).

Recent research (Styczen and Høgh-Schmidt, 1988) has suggested that kinetic energy may not be the best parameter of the rain to explain soil detachment under vegetation or on cohesive soils. A different approach is proposed in which soil detachment is proportional to the sum of the squared momenta of the raindrops:

$$\mathrm{DET} = A(2\hat{e})^{-1} Pr \sum^{\delta} N_\delta p_\delta^2, \tag{2.10}$$

where A=a soil-dependent constant of proportionality; $\hat{e}$=the average energy required to

Table 2.4 Values of squared momentum for different intensities of rain

Rainfall intensity, I (mm/h)	*Squared momentum, M_R ((Ns)^2/m^{2}s)*
5	2.66×10^{-7}
10	8.88×10^{-7}
20	2.86×10^{-6}
35	7.11×10^{-6}
50	1.25×10^{-5}
75	2.32×10^{-5}
100	3.56×10^{-5}
125	4.92×10^{-5}
150	6.38×10^{-5}
175	7.93×10^{-5}
200	9.55×10^{-5}
225	1.12×10^{-4}
250	1.30×10^{-4}

break the bonds between two micro-aggregates of soil, and the energy lost by heat in the process; Pr=the probability that the kinetic energy received by the detached micro-aggregate(s) is large enough to make it measurable as splash, i.e. to make the micro-aggregate jump a minimum distance; N_δ=the number of raindrops of size (diameter) δ; and p_δ=the drop momentum $(m_\delta \cdot v_\delta)$.

A, $\hat{e}$ and Pr are related to soil properties, while N_δ and p_δ are rainfall properties; m and v refer respectively to the mass and velocity of the raindrop.

For the Marshall-Palmer drop-size distribution, $N_\delta p_\delta^2$ is proportional to $I^{1.63}$ for $0<I<100$ mm/h and $I^{1.43}$ for $100<I<250$ mm/h. Values for the squared momentum, $M_R = N_\delta p_\delta^2$, are listed in Table 2.4.

The squared momentum of the leaf drainage (M_{RC}) can be calculated in the following way (Styczen and Høgh-Schmidt, 1986), given that the amount of leaf drainage equals $CC \cdot I \cdot [1 - (SF + IC_{\mathrm{store}})]$ and the number of drops equals $CC \cdot I \cdot [1 - (SF + IC_{\mathrm{store}})/\mathrm{vol}(\delta)]$ (equation 2.11) where vol(δ)=the volume of a drop with diameter (δ); ρ_w=the density of water; $v_{\delta H}$=the velocity of the drop as a function of its diameter (δ) and fall height (H); and vol δ) $(\rho_a^2 \pi \delta^3 v_\delta^2/6)$ listed in Table 2.5.

$$M_{RC} = \frac{CC \cdot I \cdot [1 - (SF + IC_{\mathrm{store}})]}{\mathrm{vol}(\delta)} \cdot \rho_w^2 \left[\mathrm{vol}(\delta)^2 \cdot v_{\delta H}^2\right]. \tag{2.11}$$

When the sum of the squared momenta with and without a vegetation cover are known, the

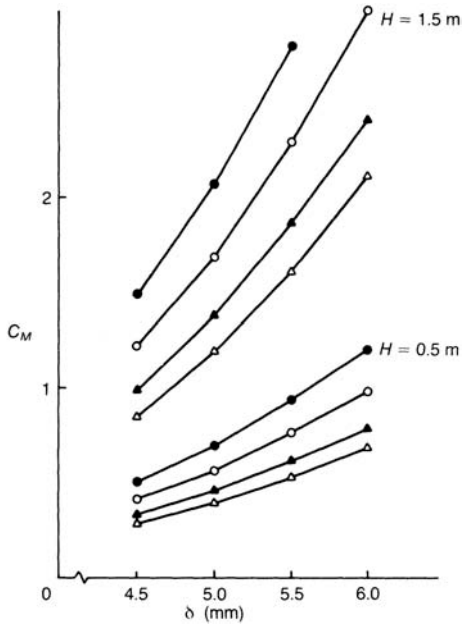

Figure 2.5 C_M as a function of the drop size of transformed rain *(δ)* for different rainfall intensities *(I)* and two canopy heights *(H)* (after Styczen and Høgh-Schmidt, 1988). The canopy cover is 100%. Storage and stemflow are estimated as 10% of the rainfall. ●, *I*=35 mm/h; ○, *I*=50 mm/h; ▲, *I*=75 mm/h; Δ, *I*=100 mm/h.

Table 2.5 Values of the parameter DH $_{(\rho_w^2 \pi \delta^3 v_0^2/6)(kg^2/ms)}$ computed for different drop sizes *(δ)* and fall heights

Fall height (m)	*Drop sizes (δ)*			
4.5 mm	*5.0 mm*	*5.5 mm*	*6.0 mm*	
0.5	0.4180	0.5734	0.7633	0.9909
1.0	0.7942	1.1002	1.4787	1.9384
1.5	1.2120	1.6890	2.2836	2.9996
2.0	1.5720	2.1866	2.9508	3.8837
3.0	2.1291	2.9998	4.0757	5.4158
4.0	2.5706	3.6229	4.9526	6.6014
5.0	2.9029	4.1470	5.6452	7.4386
6.0	3.1459	4.4763	6.0883	8.0182
7.0	3.2949	4.6733	6.3533	8.4036
8.0	3.3907	4.7957	6.5331	8.6590
9.0	3.4554	4.8971	6.6696	8.8381
10.0	3.5125	4.9769	6.7768	8.9584
13.0	3.6530	5.1843	6.9936	9.2016
∞	3.8647	5.4080	7.2934	9.5310

relative effect of the vegetation on splash (equivalent to a C-factor for splash) can be calculated as:

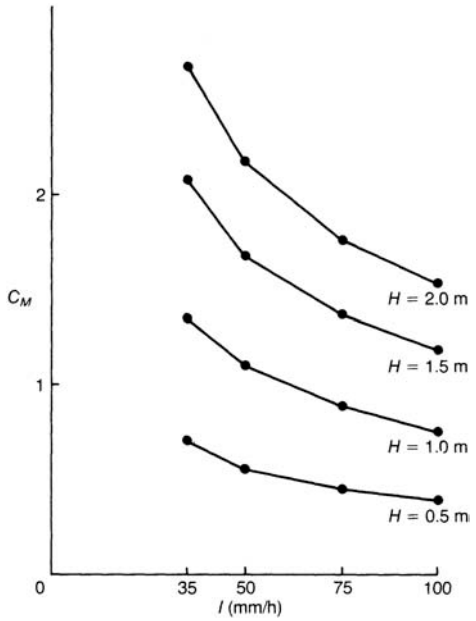

Figure 2.6 Changes in C_M with changes in rainfall intensity *(I)* for different canopy heights *(H)* (after Styczen and Høgh-Schmidt, 1988). Curves are calculated for 100% canopy cover and a drop size for leaf drainage *(δ)* of 5.0 mm.

$$C_M = \frac{(1-CC)M_R + C \cdot I \cdot (1-(SF+IC_{store})) \cdot DH}{M_R}. \quad (2.12)$$

Figures 2.5, 2.6 and 2.7 illustrate the calculated effect of different drop sizes, fall heights, stem-flow percentages and rainfall intensities on the value of C_M. Figure 2.8 shows how important the drop-size distribution of the rain can be when interpreting the effects of vegetation. As splash erosion is proportional to the drop diameter raised to the sixth power, leaf drainage may result in serious soil breakdown. Contrary to ordinary opinion, a plant canopy situated more than about 1 m above the ground cannot be expected to decrease splash erosion by itself; indeed, it is more likely to enhance it. Figure 2.9 shows this effect measured under maize (Morgan, 1985) and calculated according to equations 2.10 and 2.12.

Similar conclusions were reached by Moss and Green (1987) who, on the basis of empirical data, divided vegetation layers into the following categories:

1. Layer 1, <0.3 m: where, owing to the often high density of plant-ground contacts, leaf drainage volumes are usually small and the impact velocities too low to allow significant damage.
2. Layer 2, 0.3–1.0 m: where there is a transition from small to significant leaf drip and soil damage.
3. Layer 3, 1.0–2.5 m: from which leaf drips reach high erosivity and achieve a marked ability to cause soil damage.
4. Layer 4, 2.5–6.0 m: in which the ability of leaf drips to cause erosion and soil damage continues to increase but more slowly than in layer 3.
5. Layer 5, >6 m: where the free fall height is sufficient for leaf drips to attain 90% or more of their terminal velocity; hence, above this height there is little further increase in either their ability to cause soil damage or their erosivity.

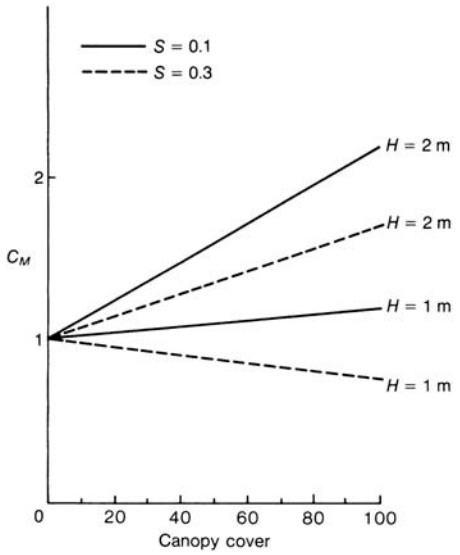

Figure 2.7 Changes in C_M with changing percentage permanent interception *(S)* for leaf drainage with a diameter *(δ)* of 5.0 mm and two heights of canopy *(H)* (after Styczen and Høgh-Schmidt, 1988). Rainfall intensity equals 50 mm/h.

If, in contrast to the above, it is assumed that splash erosion on sand is proportional to the incoming kinetic energy instead of the sum of the squared momenta, the apparent effects of vegetation become less drastic. For very tall vegetation, the energy impact approximately doubles compared to that on bare soil, but for most agricultural crops, the impact is reduced. The relative change in energy impact is shown in Figure 2.10 for four rainfall intensities, five fall heights, 10% stemflow and different cover percentages. From such calculations, a soil under a 0.5 m tall soya bean crop (80% cover, 10% stemflow) receives only 50% of the energy received by a bare soil. In the case of 1.5 m tall maize (also 80% cover and 10% stemflow), the soil receives 85–90% of the energy. For 6 m tall trees without any ground cover, the energy received by the soil reaches 200%.

It may seem strange that the amount of energy reaching the ground under trees is more than 100%. This is due to the difference in frictional resistance on small and large drops. Leaf drips are not only larger and heavier, they also gain a higher velocity so that the final impact energy is increased.

Equation 2.10 contains two soil factors that may be influenced by vegetation. These are $\hat{e}$, the average energy required to break the bonds between two micro-aggregates, and *Pr,* the probability that the kinetic energy received by the micro-aggregate is large enough to make it measurable as splash. The term, *k,* in equation 2.9, which expresses the detachability of the soil, also encompasses these factors which are discussed in more detail in section 2.4.1.

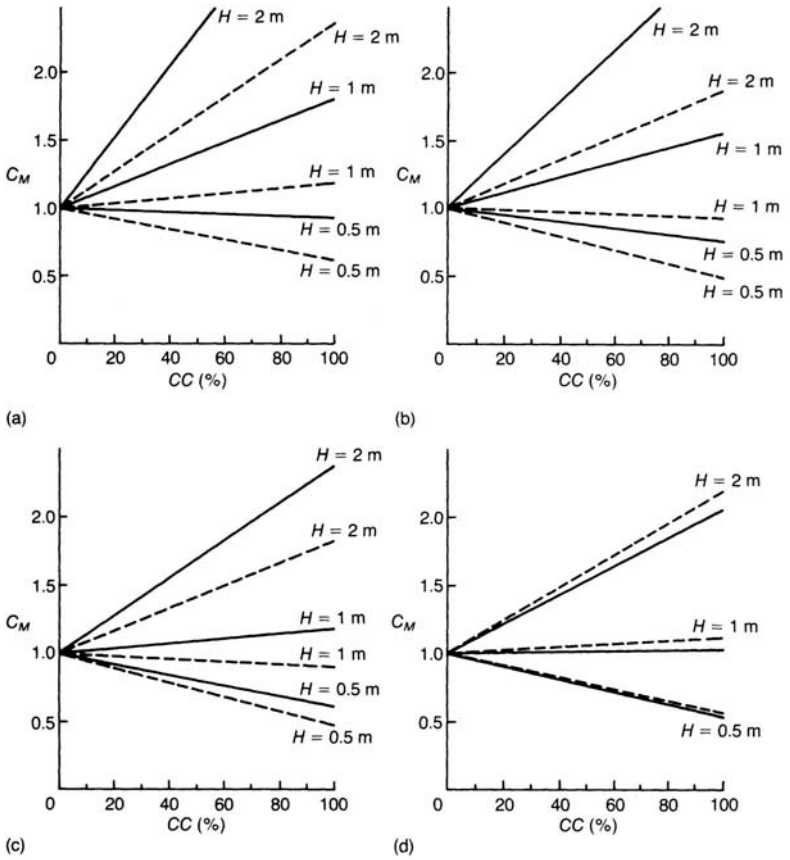

Figure 2.8 C_M as a function of percentage vegetation cover *(CC)* and canopy height *(H),* calculated for two drop-size-distributions (__, Marshall and Palmer, 1948; ----, Carter *et al.,* 1974) for leaf drainage of 5.0 mm diameter *(δ),* and percentage permanent interception storage and stemflow equal to 10% of the rainfall (after Styczen and Høgh-Schmidt, 1988). Rainfall intensities are (a) 35 mm/h; (b) 50 mm/h; (c) 75 mm/h; (d) 100 mm/h.

2.2.3 INFILTRATION

For serious erosion to take place, some amount of runoff must occur. The amount of runoff generated is closely related to the infiltration rates (unsaturated and saturated hydraulic conductivity) of the soil, the antecedent moisture content and, indirectly, to the direction of water flow within the soil.

When rain water reaches the ground underneath vegetation, it may stand a better chance of infiltrating than on unvegetated soil. Organic matter, root growth, decaying roots, earthworms, termites and a high level of biological activity in the soil help to maintain a continuous pore system and thereby a higher hydraulic conductivity. Through an increase in the infiltration rate, and perhaps also in the moisture storage capacity of the soil, vegetation may decrease the amount of runoff generated during a storm; it will probably also increase the time taken for runoff to occur. A bare soil may be compared to a bucket with few or small holes in the bottom, while the vegetated soil is rather like a slightly larger bucket with more and bigger holes. It is necessary to apply more water at a greater rate to make the second bucket overflow. Thus, a

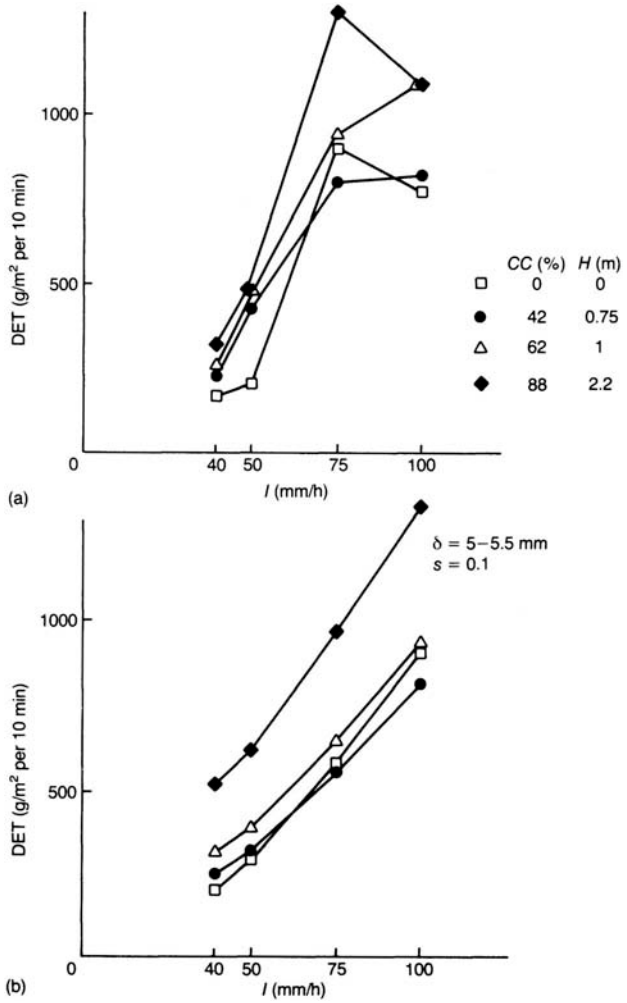

Figure 2.9 Splash erosion (DET) as a function of rainfall intensity for four combinations of percentage maize cover *(CC %)* and height *(H)* (after Styczen and Høgh-Schmidt, 1988). (a) Observed data (from Morgan, 1985); (b) calculated data. Based on equations 2.10 and 2.12 with a drop diameter *(δ)* of leaf drainage of 5.0–5.5 mm and percentage permanent interception storage and stemflow equal to 10% of the rainfall.

higher infiltration may decrease the number of erosive events per year because a greater storm is needed to produce the critical amount of runoff.

The saturated hydraulic conductivity of a soil (k_{sat}) depends on its texture and structure, the presence of cracks and the number of biopores it contains. McKeague, Wang and Coen (1986) present some guidelines for estimating k_{sat} from soil morphology. These are of interest here because the descriptions help in visualizing the changes occurring in a soil as a result of biological interference. Rawls, Brakensiek and Soni (1983) and Brakensiek and Rawls (1983) estimate k_{sat} for soils with different pore-size distri

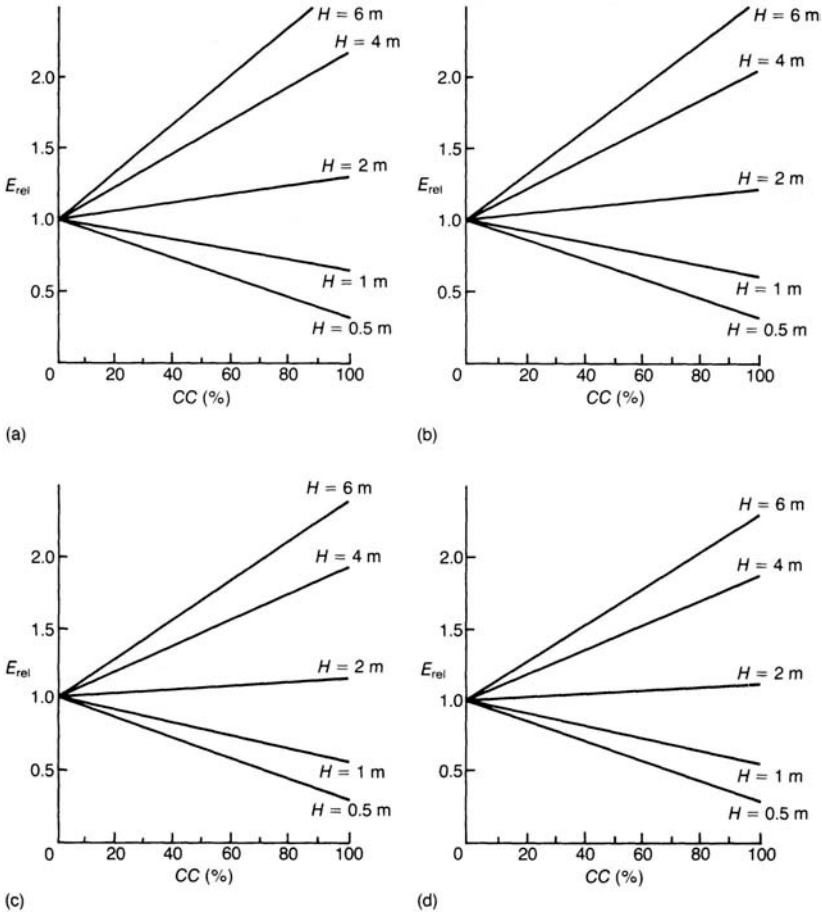

Figure 2.10 Relative change in kinetic energy of the rain (E_{rel}) reaching the soil as a function of percentage vegetation cover *(CC%)* and canopy height *(H),* calculated for the Marshall-Palmer drop-size distribution, drop diameter *(δ)* of leaf drainage of 5.0 mm and percentage permanent interception and stemflow of 10% of the rainfall. Rainfall intensities are (a) 35 mm/h; (b) 50 mm/h; (c) 75 mm/h; (d) 100 mm/h.

Table 2.6 Morphological descriptions and corresponding values of saturated hydraulic conductivity (k_{sat}) for soils with a loamy texture but different structural properties and pore content (from McKeague, Wang and Coen, 1986)

k_{sat}(mm/h)	*Soil description*
1.5–5.0	Massive to weak coarse blocky or prismatic non-compact loamy or clayey material with tightly-accommodated peds (if any), <0.02% channels >0.5 mm, and few very fine voids visible with a hand lens
5.0–15	Structureless loamy material, friable, bulk density 1.5±0.1 Mg/m^3, not compact, with <0.02% channels
15–50	*Either* moderately packed loamy to clayey material with weakly developed pedality (adherent partly-formed peds); 0.02–0.1% channels ≥0.5 mm, some of which traverse the horizon
	or moderate medium to coarse blocky loamy or clayey material with firm dense peds, <0.02% channels (=to 15 biopores/m^2 of 4 mm diameter)

k_{sat}(mm/h)	*Soil description*
50–150	*Either* approximately 0.1–0.2% channels >0.5 mm, at least half of which extend through the horizon, <0.02% large (≥5 mm) channels, structureless or weak structure; texture finer than fine sandy loam, if not compact
	or moderate fine or medium blocky with weakly adherent peds or moderate to strong medium to coarse blocky; <0.1% channels extend through the horizon; texture finer than fine sandy loam, if not compact

butions, textures and organic matter contents, with and without tillage, and with crusting.

In Table 2.6, six different morphological descriptions of loamy soil are given, together with corresponding values for saturated hydraulic conductivity (McKeague, Wang and Coen, 1986). The soils have the same texture but differ with respect to the number of biopores or the level of aggregation and structural development. According to this description, the saturated hydraulic conductivity of a loamy soil may range from 1.5 to 150 mm/h, depending on these soil characteristics.

It is evident that such large differences in hydraulic conductivity will result in large differences in the amount of runoff generated during a particular storm. Assuming that the soil is already wet and the rate of infiltration equals the saturated hydraulic conductivity of the soil, a very simple way to estimate the amount of runoff is to compare rainfall intensity and infiltration ($I-k_{sat}$). Runoff amounts for different intensities and four values of k_{sat} are given in Table 2.7. Similar results can be calculated for soils of other textures.

For dry soils, the differences in runoff generation may be even larger, as the time taken to wet the soil to saturation varies. This also implies that the delay in time before runoff occurs is longer for soils with high hydraulic conductivities.

At present it is possible to account for the effects of vegetation on infiltration only very crudely, for example by an empirical adjustment to the value of k_{sat} for an unvegetated soil, so that (Holtan, 1961):

$$k_{satveg} = k_{sat} + a^{1.4}, \tag{2.13}$$

Table 2.7 Runoff amounts (m^3/ha h) calculated for eight rainfall intensities and four infiltration rates

	Infiltration rate (mm/h)			
Rainfall intensity (mm/h)	*1.5*	*5.0*	*15*	*50*
10	85	50	0	0
20	185	150	50	0
30	285	250	150	0
40	385	350	250	0
50	485	450	350	0
75	735	700	600	250
100	985	950	850	500
150	1485	1450	1350	1000

Table 2.8 Basal areas for different vegetation types (after Holtan, 1961)

Land use or cover	*Hydrological condition*	*Percentage basal area rating*
Fallow (after row crop)	–	0.10
Fallow (after sod)	–	0.30

Land use or cover	*Hydrological condition*	*Percentage basal area rating*
Row crops	poor	0.10
	good	0.20
Small grain	poor	0.20
	good	0.30
Hay (legumes)	poor	0.20
	good	0.40
Hay (sod)	poor	0.40
	good	0.60
	excellent	0.80
Pasture or range (bunch grass)	poor	0.20
	fair	0.30
	good	0.40
Temporary pasture (sod)	poor	0.40
	fair	0.50
	good	0.60
Permanent pasture or meadow (sod)	poor	0.80
	good	1.00
Woods and forest	–	1.00

where k_{satveg}=the saturated hydraulic conductivity of the soil with a vegetation cover; and a=percentage basal area of the vegetation.

Typical values of a are given in Table 2.8. This adjustment alters k_{sat} largely as a function of vegetation density and, broadly, lumps together all the effects of vegetation mentioned above that lead to higher infiltration rates and, probably, though it is by no means clear, to a reduction in the amount of rain reaching the ground after interception by the vegetation canopy. It does not take account of the effect of the vegetation cover on the spatial distribution of the rainfall at the ground surface which, through concentrations of water in leaf drips and stemflow, can lead, as seen above, to localized intensities which may exceed infiltration capacity and result in runoff generation. Alter natively, k_{satveg} could be measured in the field but it is often difficult to place infiltrometers over representative areas of the vegetation cover, particularly with shrubs and scrub. Also, the variability in k_{satveg} is invariably great, with coefficients of variation in excess of 200%, so that large numbers of replicates are required to obtain meaningful values.

A further way in which vegetation influences infiltration is through the difference in antecedent moisture content that may occur because more water is removed by evapotranspiration from a soil covered by vegetation than from a bare soil surface. Thus, the capillary pressure, ψ, within the soil at the onset of rain may be lower (ψ numerically higher) and the time before saturation is reached longer for a vegetated soil.

2.2.4 SURFACE CRUSTING

On silty soils, soils containing high proportions of fine sand, soils low in organic matter and soils which for some other reason have an unstable or poor structure, surface crusting or sealing may take place, as the finer particles detached by raindrop impact clog up the pores and cracks and reduce the infiltration rate. The

speed of crusting seems to be related to either the incoming shear forces of the raindrops (Farres, 1978; Al-Durrah and Bradford, 1982) or the rainfall energy (Boiffin, 1985; Govers and Poesen, 1985).

The effect of raindrop impact on infiltration can be particularly spectacular on soils susceptible to crusting. Brakensiek and Rawls (1983) present data on soils with and without crusts, where the crusted soils sustain infiltration rates 15–20 mm/h lower than the uncrusted soils. Measurements on sandy soils in Israel show that crusting reduces the infiltration capacity from 100 to 8 mm/h, and on a loess soil from 45 to 5 mm/h (Morin, Benyamini and Michaeli, 1981). The infiltration capacity of sandy soils in Mali ranges from 100 to 200 mm/h but, when a crust has developed, it is reduced to 10 mm/h. Only a few storms are needed to bring about this change. A 50% reduction in infiltration can occur in one storm (Hoogmoed and Stroosnijder, 1984). Studies on the behaviour of loamy soils in northern France (Boiffin, 1985) show that surface crusting can reduce infiltration capacities from 20–50 mm/h to about 1 mm/h at a rate which is dependent upon the cumulative rainfall received since tillage.

Considering the effect of vegetation on the rainfall energy (Figure 2.10), it may be expected that the speed at which the infiltration rate is reduced is altered by a plant cover. Under relatively low vegetation, the infiltration may remain higher for a longer time than on bare soil, resulting in runoff occurring later and in smaller quantities. Under tall vegetation without undergrowth, the opposite situation may prevail, because sealing or crusting will take place shortly after the onset of rain.

2.3 HYDRAULIC EFFECTS

The passage of water across a bare soil surface may entrain and transport soil particles already detached and, particularly if the flow is concentrated in channels, may also detach additional particles. Erosion is said to be either detachment-limited or transport-limited, depending on how much detached material is available for transport at a given moment. If too much material exists, all of it will not be removed, the erosion rate will be controlled by the transport capacity and the erosion will be transport-limited. If the transport capacity exceeds the detachment rate, all the detached particles will be removed, the erosion rate will be controlled by the supply of detached material and will be detachment-limited.

Flow transport capacity and detachment by flow are often easily confused. Both are related to energy-spending processes within the flow at the interface between the flowing water and the bed. There are differences, however, in the way the energy is expended. Transport capacity is defined as the capacity of flow to carry material of a given noncohesive type (primary particles and individual soil aggregates) with the energy of the flow spent on lifting and carrying the sediment particles. Soil detachment by flow relates to the situation where the energy of the flow is spent on detachment as well as entrainment and transport of sediment particles. Vegetation can limit the capacity of flowing water to detach and transport sediment. The most obvious effect is through the reduction in flow velocity brought about by contact between the flow and the vegetation. The stems and leaves of the vegetation impart roughness to the flow.

2.3.1 SURFACE ROUGHNESS AND FLOW VELOCITY

Surface roughness is an important parameter controlling the speed of the generated runoff. It may be described by a coefficient of friction. The coefficient of friction is usually an ‘effective’ roughness coefficient that includes the effects of raindrop impact, concentration of the flow, obstacles such as litter, ridges, rocks and roughness from tillage, the frictional drag over the surface, and the erosion and transport of

sediment (Engman, 1986). It is more a function of vegetation (plant arrangement, plant population, litter, mulch) and, on agricultural land, tillage methods, than it is a soil-vegetation interaction parameter. The roughness coefficient is normally considered as a summation of the roughness imparted by the soil particles, surface micro-topography (form roughness) and vegetation, acting independently of each other.

Surface roughness is inversely related to both the velocity and quantity of runoff as expressed by the following equations:

$$u = R^{0.667} S^{0.5} / n \tag{2.14}$$

and

$$Q = R^{1.667} S^{0.5} / n \tag{2.15}$$

where u=the velocity of the flow (m/s); R=the hydraulic radius (m), often taken as equal to flow depth in shallow flows; S=slope of the energy line (m/m); n=Manning's roughness coefficient ($m^{1/6}$); and Q=the quantity of runoff (m^3/ms).

Rewriting the equations shows that velocity is dependent on roughness to the power of −0.6 ($u \propto n^{-0.6}$).

For a given amount of runoff it may be calculated that doubling the roughness increases the water depth by 50% and decreases velocity by 34%.

Alternative friction factors to Manning's n are the dimensionless Darcy-Weisbach *(f)* and Chezy's *(C)*. These are related to Manning's n and to each other as follows:

$$f = 8 g n^2 R^{-0.33} \tag{2.16}$$

$$C = R^{0.167} / n \tag{2.17}$$

and

$$C = (8g/f)^{0.5}. \tag{2.18}$$

Engman (1986) has suggested a number of values for Manning's roughness coefficient. These are listed in Table 2.9. The possible range of n is large: for bare smooth soil, n is in the order of 0.01; for 5–10 t/ha of straw mulch, n=0.07; and for grass, n ranges from 0.2 to 0.4. Thus, for a constant amount of runoff, surface roughness reduces flow velocity on a mulched field to approximately one-third and on a grass field to one-eighth of what it would be on bare smooth soil.

The level of roughness depends upon the morphology of the plant and its density of growth. Manning's n values can be related to a vegetation retardance index *(CI)* which is a function of the density and height of the plant stems (Temple, 1982; Table 2.10). The range in n values for each retardance class reflects the variation in roughness which occurs with flow depth (Figures 2.11 and 2.12). With shallow flows, the vegetation stands relatively rigid and roughness values are about 0.25–0.3, associated with distortion of the flow around the individual plant stems. As flow depth increases, the stems begin to oscillate, further disturbing the flow, and roughness values rise to around 0.4. When flow depth begins to submerge the vegetation, roughness values decline rapidly, often by an order of magnitude, because the plants tend to lay down in the flow and roughness is mainly

Table 2.9 Recommended values for Manning's n (after Engman, 1986)

Cover or treatment	*Residue rate (t/ha)*	*Value recommended*	*Range*
Concrete or asphalt		0.011	0.01–0.013
Bare sand		0.01	0.010–0.016
Gravelled surface		0.02	0.012–0.03
Bare clay-loam (eroded)		0.02	0.012–0.033
Fallow—no residue		0.05	0.006–0.16

Cover or treatment	*Residue rate (t/ha)*	*Value recommended*	*Range*
Chisel plough	<0.6	0.07	0.006–0.17
	0.6–2.5	0.18	0.07–0.34
	2.5–7.5	0.30	0.19–0.47
	>7.5	0.40	0.34–0.46
Disc/harrow	<0.6	0.08	0.008–0.41
	0.6–2.5	0.16	0.10–0.25
	2.5–7.5	0.25	0.14–0.53
	>7.5	0.30	–
No tillage	<0.6	0.04	0.03–0.07
	0.6–2.5	0.07	0.01–0.13
	2.5–7.5	0.30	0.16–0.47
Mouldboard plough		0.06	0.02–0.10
Coulter		0.10	0.05–0.13
Range (natural)		0.13	0.01–0.32
Range (clipped)		0.10	0.02–0.24
Grass (blue grass sod)		0.45	0.39–0.63
Short grass prairie		0.15	0.10–0.20
Dense grass		0.24	0.17–0.30
Bermuda grass		0.41	0.30–0.48

due to skin resistance; as a result, velocities increase.

Greatest reductions in flow velocity occur with dense, spatially uniform vegetation covers. Very open, clumpy and tussocky vegetation is less effective and may even lead to localized increases in velocity and erosion as flow becomes concentrated between the clumps. Figure 2.13 shows typical flow paths around a clump of vegetation. As flow separates around the clump, pressure (normal stress) is higher on the upstream than on the downstream face, and eddying and turbulence are set up downstream; in addition, a zone of backflow is established just upstream of the clump (Babaji, 1987). Vortex erosion can occur both upstream and downstream. The combined effect of these processes means that erosion rates under tussocky vegetation may remain high and match those prevailing on bare soil (De Ploey, Savat and Moeyersons, 1976).

2.3.2 SEDIMENT TRANSPORT CAPACITY

A number of equations have been proposed for calculating the transport capacity of flow. Traditionally, transport capacity has been defined with respect to sandy beds (river beds) and some confusion arises when dealing with cohesive beds, partly because energy is also spent in detaching the material and partly because the mechanisms of detachment are less well understood than is the case with sand particles.

Table 2.10 Values of Manning's *n* for different vegetation retardance classes (after Temple, 1982)

Vegetation type	*CI*[a]	*n*
Very tall dense grass (>600 mm)	10.0	0.06–0.20

Vegetation type	*CI*[a]	*n*
Tall grass (250–600 mm)	7.6	0.04–0.15
Medium grass (150–250 mm)	5.6	0.03–0.08
Short grass (50–150 mm)	4.4	0.03–0.06
Very short grass (<50 mm)	2.9	0.02–0.04

[a] *CI*=index of vegetation retardance defined by Temple, (1982):

$$CI = 2.5\left(h\sqrt{M}\right)^{1/3}$$

where h is the height of the plant stems (m) and M is the density of stems (stems/m^2).
Reference stem densities for good uniform stands are:

Bermuda grass	5380
Buffalo grass	4300
Kentucky bluegrass	3770
Weeping love grass	3770
Alfalfa	5380
Common lespedeza	1610
Sudan grass	538

For legumes and large-stemmed or woody species, the reference stem density is about five times the actual count of stems very close to the bed.

The situation is complicated further because at least three main modes of transport may occur in the flow. Material may be transported as bed load, suspended load or wash load. Bed load is transported in a rolling manner along the soil surface. This mode of transport dominates when the ratio between the lifting forces and the stabilizing forces on the particle is below 0.2; in other words, when the particles are large and heavy compared to the forces within the flow. When this ratio is greater than 1.0, particles are transported as suspended load (Engelund and Hansen, 1967). For very small particles (less than approximately 2 μm), Brownian movements dominate over sedimentation following Stokes' Law, and this material is referred to as wash load.

A very large number of sediment transport equations have been published. Some were derived for sandy river beds, others for soils, but none covers all three modes of transport. The following are typical of those in which sediment transport is related to runoff.

Schoklitsch (1950): for bed load in rivers,

$$Qs = CsS^{1.4}\gamma_w^2 Q^{0.6}\left(Q^{0.6} - Qc^{0.6}\right)n^{-0.5}, \tag{2.19}$$

where Cs=a coefficient expressing soil characteristics: γ_w=unit weight of water; and Q_c is

Table 2.11 Relative transport capacities (m^3/m s) for runoff generated on loamy soil with different hydraulic properties. The runoff amounts used are given in Table 2.7

	Saturated hydraulic conductivity (mm/h)			
Precipitation (mm/h)	*1.5*	*5.0*	*15*	*50*
10	0.055	0.023	0	0
20	0.20	0.14	0.023	0
30	0.41	0.33	0.14	0

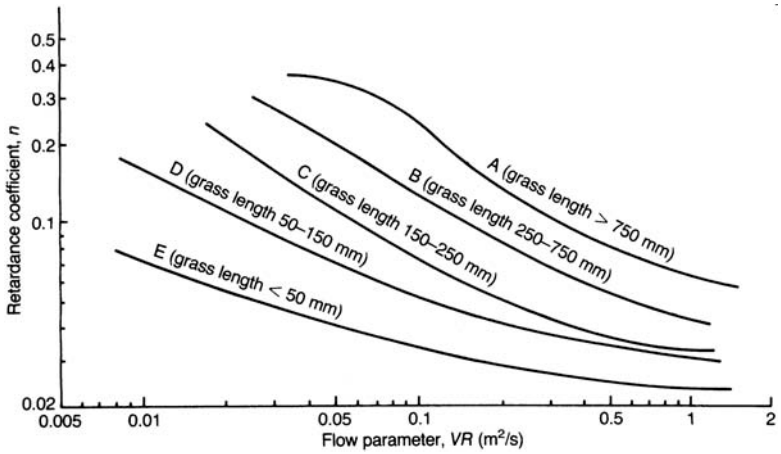

Figure 2.11 Variation in the frictional resistance of grass swards expressed by Manning's *n* for different retardance categories (after US Soil Conservation Service, 1954).

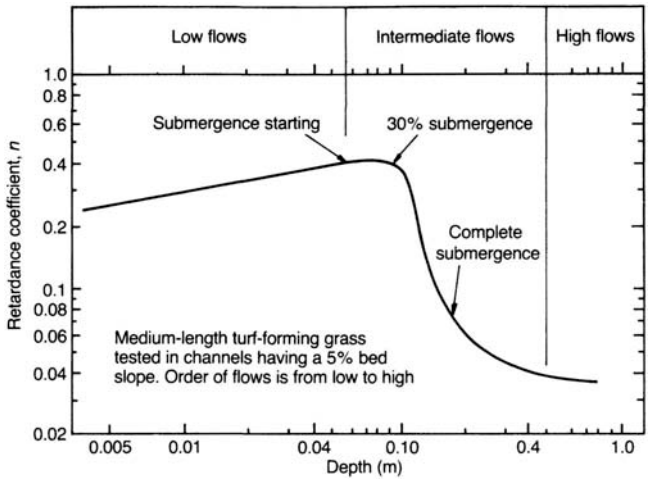

Figure 2.12 Relationship between Manning's *n* and depth of water flow for a medium length grass (after Ree, 1949).

	Saturated hydraulic conductivity (mm/h)			
Precipitation (mm/h)	*1.5*	*5.0*	*15*	*50*
40	0.68	0.58	0.33	0
50	1.0	0.88	0.58	0
75	2.0	1.8	1.4	0.33
100	3.3	3.1	2.5	1.1
150	6.5	6.2	5.5	3.3

the critical discharge at which sediment transport takes place.

Meyer and Wischmeier (1969): for shallow flows on hillslopes,

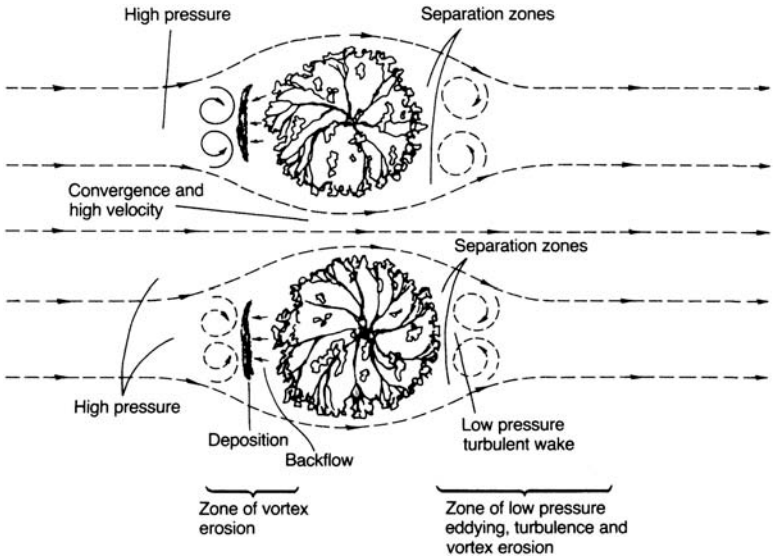

Figure 2.13 Plan view of the pattern of water flow around tussocky vegetation (after Babaji, 1987).

$$Qs = kS^{5/3}Q^{5/3}, \tag{2.20}$$

where k=an experimental coefficient largely related to soil characteristics.

Engelund and Hansen (1967): for bed load transport in rivers but applied by Nielsen and Styczen (1986) to runoff on hillslopes,

$$Qs = 0.04(2g/0.25f)^{1/6}(QS)^{5/3}/(J-1)^2 g^{1/2} d_{50}, \tag{2.21}$$

where f=Darcy-Weisbach roughness coefficient; J=relative sediment density, defined as the ratio γ_s/γ_w, where γ_s is the volume weight of transported sediment; and d_{50}=the diameter at which 50% of the soil particles are finer.

De Ploey (1984): for overland flow and rill flow on hillslopes,

$$Qs/Q \propto S^{1.25}Q^{0.625}. \tag{2.22}$$

Govers and Rauws (1986): for overland flow,

$$Qs/Q = ASu + B, \tag{2.23}$$

where Su=unit stream power (product of slope and mean flow velocity); and A, B=empirical coefficients which vary in value with sediment particle size.

Carson and Kirkby (1972): for overland flow,

$$Qs = 0.0085Q^{1.75}S^{1.625}d_{84}^{-1.11} \tag{2.24}$$

where d_{84}=the diameter at which 84% of the soil particles are finer.

Morgan (1980): for overland flow,

$$Qs = 0.0061Q^{1.8}S^{1.13}n^{-0.15}d_{35}^{-1}, \tag{2.25}$$

where d_{35}=the diameter at which 35% of the soil particles are finer.

In these equations, Qs=sediment transport capacity (m^3/m s) and Q=volume of runoff (m^3/m s), so that Qs/Q=sediment concentration.

Despite their differences and shortcomings, the equations consider transport capacity to be proportional to the volume of runoff raised to the power of between 1.6 and 1.8, or to *Q(Su−B)*. Transport capacity is also inversely related to both roughness, *n,* raised by powers of between 0.15 and 0.5, and particle size, raised by the power of approximately 1. As indicated above, vegetation will affect the transport capacity of runoff by controlling its volume and, through the effect on surface roughness, its velocity.

As an example of the type of calculations that can be made using the above equations, Table 2.11 lists some relative transport capacities calculated using the Engelund-Hansen equation for the runoff amounts given in Table 2.7. The values are approximate and are presented only to show the differences in transport capacity that may arise from differences in infiltration rates. The effects of soil properties on transport capacity are discussed in section 2.4.

In reality, the calculation of transport capacity is much more complicated because the sediment consists of a mixture of primary particles and soil aggregates of different sizes. For soils with a wide aggregate-size distribution, the single particle-size parameter included in the above equations is inadequate, and the transport capacity may have to be calculated separately for different particle or aggregate size classes. For a small amount of runoff, the area of 'attack' is limited to the area covered by small particles. When the runoff increases, more particle sizes and thus a larger surface area become accessible. When an increasing amount of fine material is removed from the surface and only the larger particles are left behind, hardly any material can be removed because the larger particles protect the soil surface. This effect is called armouring.

2.3.3 SOIL DETACHMENT BY FLOW

Soil detachment by flow is often considered as a function of the shear stress of the flow ($\tau = \rho_w g S Q$), raised to the third or fifth power, or as a linear function of the shear stress above a critical value $u_m = 1/n R_s^{2/3} S_g^{1/2}$; which is related to the shear strength of the soil (τ_s). One example of an equation based on this view is:

Rose *et al.* (1983),

$$DF = 0.276\eta(\rho_w g S Q - \tau_s), \tag{2.26}$$

where *DF*=the rate of soil particle detachment by flow, and η=the efficiency of bedload transport.

Alternatively, detachment is viewed as a function of the grain shear velocity *(u*g)* above a critical value (u^*g_{crit}) which is dependent upon the cohesion of the soil. Total shear velocity (u^*) of the flow is defined by:

$$u^* = (gRS)^{0.5} \tag{2.27}$$

and the grain shear velocity represents that portion which is associated with the roughness of the soil grains. The remaining shear velocity relates to microtopographic (form) roughness and the vegetation. The following equation is an example of this approach.

Rauws and Govers (1988):

$$DF = A(u^*g - u^*g_{crit}), \tag{2.28}$$

where *A*=a coefficient expressing soil, including grain size characteristics, and

$$u^*g_{crit}(\mathrm{cm/s}) = 0.89 + 0.56c, \tag{2.29}$$

where *c*=cohesion of the soil (kPa) at saturation as measured with a torvane.

Several authors (Meyer and Wischmeier, 1969; Foster and Meyer, 1975; Beasley, Huggins and Monke, 1980; Park, Mitchell and Scarborough, 1982) consider that the detached material fills up the transport capacity of the flow and that sedimentation occurs only when the flow is overloaded. Alternatively, it might be assumed that the detached material settles continuously and that the amount present in the flow

represents a balance between detachment and sedimentation (Rose *et al.* 1983; Nielsen and Styczen, 1986). The net effect when the situation is viewed as a balance of processes is described by the following equation:

$$DF = \eta Q s_{EH}, \tag{2.30}$$

where $=\eta$ is the ratio of energy spent by the flow on lifting particles to the total amount of energy spent on lifting plus detachment; and Qs_{EH}=flow transport capacity calculated according to Engelund and Hansen (equation 2.21). Equation 2.26 (Rose *et al.* 1983) follows the same line of reasoning but is derived in a different way.

On the basis of laboratory tests with sandy, clay loam and clay soils and with sand, Quansah (1985) obtained the empirical relationship:

$$DF = e^{16.37} Q^{1.5} S^{1.44} d_{50}^{-1.54}, \tag{2.31}$$

where DF is in kg/m^2, Q in m^3/m s and d_{50} in mm.

These equations show that whether detachment by flow is described by itself or sedimentation is included, the quantity of runoff generated plays an important role. The effect of runoff, as measured by the value of the power exponent, is greatest when sedimentation is considered. The empirically derived value of 1.5 (equation 2.31) is closer to the value of 1.67 (equation 2.30) suggested when sedimentation is taken into account than to the value of 1.0 (equation 2.26) when it is not. Inclusion of sedimentation may therefore be the most promising approach.

As described earlier, differences in interception and infiltration due to vegetation will have an important influence on runoff generation and, therefore, on detachment by flow. Roughness is accounted for only in equation 2.30. According to this equation, doubling the roughness will decrease the amount of detachment by 20% for a given quantity of runoff.

2.3.4 TRANSPORT OF SPLASHED MATERIAL

Splash erosion may take place in the absence of runoff. However, the amount of material removed from a hillslope or a catchment in this manner is very small, even though it may be the dominant erosion process where runoff amounts are negligible.

When runoff occurs, the transport of the splashed particles depends upon the quantity of the splashed material which goes into the flow and on the flow velocity. Viewed in a very simple manner, splashed material, except for very small particles, behaves as suspended load and moves with the water until it settles. The average fall height will be a function of water depth, D (e.g. $D/2$, because the splashed material could be rather evenly distributed due to turbulence). The time (t) taken to settle becomes $D/2w$, where w is the average fall velocity of a particle of a given size and density. The distance moved by this particle becomes $t \cdot u = uD/(2w) = Q/(2w)$ (Styczen and Nielsen, 1989).

The distance upstream from which splashed material is transported over a given point thus varies with runoff quantity, particle size and particle density. The greater the velocity of runoff generated, the more splashed material is likely to be moved out of an area. The larger the amount of detachment, the greater will be the speed of sedimentation and the shorter the distance moved by the detached particle. Thus infiltration and surface roughness, through their effects on runoff generation, are important controls over the splash process.

However, if the soil surface is totally covered by water of some depth, splash does not take place at all. Relations suggested by Park, Mitchell and Scarborough (1982) and Rose *et al.* (1983) indicate that with a water depth of 6–8 mm and raindrops of 2.0–2.5 mm, splash is reduced by 80–90% compared with that for

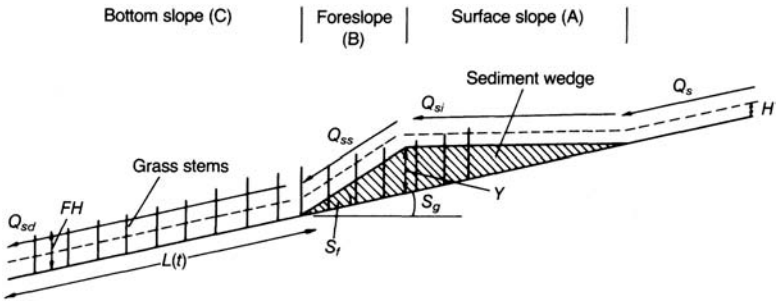

Figure 2.14 Schematic representation of sedimentation in a grass filter strip. Q=runoff; H=flow depth; Y=height of sediment wedge; FH=height of the grass in the filter; S_g=ground slope; S_f=foreslope of sediment wedge. Other notation described in the text (after Hayes, Barfield and Tollner, 1984).

zero water depth. Equation 2.9 proposes that splash decays exponentially with increasing water depth. Vegetation in contact with the soil surface can increase water depths by reducing flow velocity.

2.3.5 SEDIMENTATION

Vegetation not only retards flow but acts as a filter to sediment being carried in the flow. The denser the vegetation, the more sediment can be trapped and removed from the flow. The effectiveness of close-growing vegetation in causing sedimentation has been modelled for grass barriers using laboratory experiments (Tollner, Barfield and Hayes, 1982; Hayes, Barfield and Tollner, 1984). The sediment wedge created by the barrier consists of three zones (Figure 2.14): (A) the surface slope, (B) the foreslope, and (C) the bottom slope. As the sediment is trapped and the sediment wedge builds up, these zones migrate downslope or downstream.

The model is most easily understood by starting with zone C and calculating its trapping efficiency (fC) over time (t):

$$f\mathrm{C}(t) = \exp - 1.05 \times 10^{-3}(u_m \cdot R_s)/\nu)^{0.82} (w \cdot L(t)/u_m \cdot H)^{-0.91}, \quad (2.32)$$

where $f(\mathrm{C}) = (Q_{sd} - Q_{so})/Q_{sd}$; Q_{so}=sediment outflow from the filter; Q_{sd}=sediment trans port over zone C; $u_m = 1/nR_s^{2/3}S_g^{1/2}$; $R_s = (SS \cdot H)/(2H + SS)$;; ν=kinematic viscosity of the water; w=settling velocity of the sediment; $L(t)$=length of zone C along the slope; S_g=slope of the ground surface; SS=average spacing of the grass stems; H=depth of flow; and n=a modified Manning's n (S/cm$^{1/3}$) approximated as 0.012 for grass stems.

This relationship is based on an application of the Manning equation of flow velocity using an analogy between flow in a rectangular channel and flow between grass stems to give a channel with a width equal to the average spacing of the stems. The critical factors determining the efficiency of the filter are the density, shape and resilience of the grass stems as these affect the surface roughness. The hydraulic radius (R_s) is defined here as the spacing hydraulic radius.

The term Q_{sd} is estimated using an Einstein-type sediment transport equation:

$$\Delta(d/S_g R_s) = 1.08(Q_{sd}/(\gamma_s \Delta g\, d^3))^{-0.28}, \quad (2.33)$$

where $\Delta = (\gamma_s - \gamma_w)/\gamma_s$.

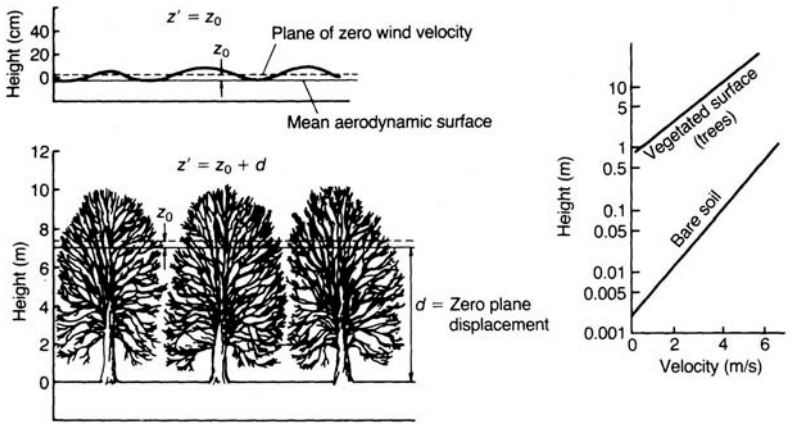

Figure 2.15 Wind velocity as a function of height above a bare and a vegetated soil surface.

Knowing Q_{sd} and the right-hand side of equation 2.32, the sediment outflow (Q_{so}) and the trap efficiency (fC) are determined.

Sediment transport over zone B (Q_{ss}) is represented by:

$$Q_{ss} = (Q_{si} - Q_{sd})/2, \tag{2.34}$$

and the trapping efficiency of zone B (fB) is calculated from:

$$f\mathrm{B} = (Q_{si} - Q_{sd})/Q_{si}. \tag{2.35}$$

The term Q_{ss} is estimated using equation 2.33 but substituting Q_{ss} for Q_{sd} and S_f (slope of the foreslope of the sediment wedge) for S_g.

Sediment transport over the surface slope of zone A is represented by Q_{si} and the mass deposition rate for the wedge is Q_{su}. Then

$$Q_{si} = Q_s - Q_{su}, \tag{2.36}$$

$$Q_{su} = (\gamma_{\mathrm{sdep}}(Y_f^2 - Y_i^2))/(2(t_f - t_i)S_g), \tag{2.37}$$

$$Y_f(t) = \mathrm{FH} \qquad \text{for } Y_f(t) \geqslant \mathrm{FH}, \tag{2.38}$$

$$Y_f(t) = (2/\gamma_{\mathrm{sdep}}(f\mathrm{B} \cdot Q_{si} \cdot S_e)(t_f - t_i) + Y_i(t)^2)^{1/2} \qquad \text{for } Y_f(t) < \mathrm{FH}, \tag{2.39}$$

where Qs=sediment transport upslope of the barrier; Y=height of the sediment wedge; $(t_f–t_i)$=difference in time between time periods f and i; γ_{sdep}=unit weight of deposited sediment; S_e=angle between foreslope of the sediment wedge and the ground slope; and FH=height of the grass in the filter.

The extent of the sediment wedge upslope (Z_f) is calculated from:

$$Z_f = Y_f/S_g. \tag{2.40}$$

The total amount of sediment trapped in the filter (T) is determined from:

$$T = Q_{su} + (Q_{sd} - Q_{so}) + (Q_{si} - Q_{sd}). \tag{2.41}$$

The trapping efficiency of the filter is:

$$f = (Q_s - Q_{so})/Q_s. \tag{2.42}$$

In addition to the properties of the grass stems mentioned above, the effectiveness of the filter will depend upon the height of the grass as this will influence the volume of sediment that can be trapped.

Sedimentation in the filter causes slope steepness to decline as the ground slope is replaced by the slope of zone A in the sediment wedge. Flow velocities are thus decreased and the erosive capacity of the flow reduced. However, the foreslope of the sediment wedge is steeper than the ground slope. Whilst the foreslope remains within the barrier, the potential increase in velocity over this steeper slope is largely offset by the roughness imparted by the grass stems. When the foreslope has migrated downslope to the edge of the barrier, however, flow leaving the barrier will have its velocity increased. Since, as shown in laboratory experiments by Emama (1988), most of the sediment originally carried in the flow is deposited within and upslope of the barrier, the flow is now largely sediment free and is therefore able to effect considerable erosion.

2.3.6 MODIFICATION OF AIR FLOW

Shear velocity in open ground

In the absence of convective eddies generated by vertical temperature gradients, wind speed over uniform level open ground increases logarithmically with height from a height (z_0) which is defined as the height above the mean aerodynamic surface at which wind velocity is zero (Figure 2.15). According to Bagnold (1941), the open field wind velocity profile is described by the equation:

$$u(z) = 2.3/k \cdot u^* \cdot \log(z/z_0), \tag{2.43}$$

where u=mean wind velocity at height z; k=von Karman universal constant for turbulent flow (=0.4 for clear fluids); and u*=drag or shear velocity.

The term z_0 is known as the roughness length and is a measure of the ground surface roughness. Bagnold (1941) found that z_0 was equal to

Table 2.12 Drag coefficients for resistance of vegetation in moving air (after Wright and Brown, 1967; Randall, 1969; Voetberg, 1970; Morgan and Finney, 1987)

Cover	*z_0(cm)*	*CD*	*Cd*
Grass	0.2–0.3	0.005–0.009	
Sugar beet	0.4–1.6		0.003–0.33
Wheat	1.2–3.0		0.001–0.08
Barley			0.001
Planted straw strips	2.1		0.001–0.08
Onions	0.8		0.006–0.50
Peas	0.4		0.001–0.23
Potatoes	5.4		0.001–0.07
Broad beans			0.01–0.05
Apple orchard (winter)		0.02–0.03	
Apple orchard (summer)		0.06–0.07	
Maize		0.01–0.10	0.02–0.15
Rice		0.01–0.10	

Cover	z_0*(cm)*	*CD*	*Cd*
Coniferous forest	1.0	0.03–0.10	
Deciduous forest	1.8	0.01–0.03	

z_0, *CD* and *Cd* are defined in the text.
Values for *Cd,* except for maize, are for crop biomass in the lower 5 cm of the atmosphere and for a wind velocity at 5 cm height of 1 m/s.
The values of z_0, *CD* and *Cd* shown here are typical for the cover types specified. In practice, values of z_0 decrease with increasing wind velocity whereas those of *CD* and *Cd* can both increase and decrease with increasing wind velocity. Values of all three coefficients increase with increasing plant growth.

about 1/30th of the height of the sand particles or stones that caused the roughness. Other workers, however, indicate that z_0 approximates 1/10th of the height of the roughness elements (Monteith, 1973; Bache and MacAskill, 1984).

The shear velocity can be calculated by rear-ranging equation 2.43. It is thus directly proportional to the rate of increase in wind velocity with the logarithm of height. Since it is equivalent to the slope of the line in Figure 2.15, it can be determined by measuring the wind speed at two different heights, plotting the results on a graph of velocity versus the logarithm of height, joining the points with a straight line and calculating the slope of the line expressing the change in velocity for a unit change in log height. It should be noted that the convention of plotting the dependent variable on the *y*-axis gives way to the convention of plotting height vertically. Thus, higher shear velocities appear as gentler-sloping lines on the graph since they represent a high value of change in the *x*-axis for a unit change in the *y*-axis.

Shear velocity is not an actual velocity but has the same units as velocity. It is defined by

$$u^* = \tau/\rho_a, \qquad (2.44)$$

where τ=surface shear stress exerted by the air flow; and ρ_a=density of the air (=0.00123 Mg/ m^3 as an average value at sea-level).

Shear velocity with vegetation

Vegetation reduces the shear velocity of the wind by exerting a drag on the air flow. This is compensated for by a transfer of momentum from the air to the vegetation which, for an incompressible fluid, implies a reduction in velocity. Vegetation thus acts as a momentum sink. Vegetation increases the roughness length, z_0, which can be approximated in value as 1/10th of the height of the plant canopy. Typical values of z_0 for a range of surfaces are given in Table 2.12. A vegetation cover also displaces the height of the mean aerodynamic surface above the ground by a distance, *d,* known as the zero plane displacement (Figure 2.15). The value of *d* is usually approximated as 0.7 times the height of the plant canopy. Wossenu Abtew, Gregory and Borrelli (1989) have shown that a more accurate assessment can be obtained from $d=H\times F$, where *H* is the average height of the individual roughness elements and *F* is the fraction of the total surface covered by those elements. They also show that the roughness length can be estimated from $z_0=0.13\ (H-d)$. The term z_0 may be viewed as a measure of the bulk effectiveness of the vegetation cover in absorbing momentum, and the term *d* is a measure of the mean height at which the absorption takes place (Thom, 1975).

Drag coefficients

The frictional drag exerted on the atmosphere by a vegetation canopy in bulk can be expressed by an equation derived from a simplification of the Navier-Stokes equation for the conservation of momentum in incompressible, steady, two-dimensional air flow (Seginer, 1972; Skidmore and Hagen, 1977; Hagen *et al.,* 1981):

$$\tau = 1/2\rho_a u(z)^2 CD, \tag{2.45}$$

where τ=the drag force per unit horizontal area of vegetation; and CD=a bulk drag coefficient.

Equating the expressions of τ in equations 2.44 and 2.45 gives:

$$CD = 2u^{*2}/u(z)^2. \tag{2.46}$$

Considering this equation alongside equation 2.43, it is clear that a relationship exists between the bulk drag coefficient and the aerodynamic properties of the crop canopy as expressed by z_0 and d. In general terms, the rougher the surface and the higher the zero plane displacement, the greater is the drag coefficient. Since both z_0 and d vary with vegetation type and its stage of growth, the drag coefficient, *CD,* will also vary. All three terms are also dependent upon wind speed. As wind velocity increases, *CD* and z_0 should fall as a result of streamlining of the foliage elements downwind and d will fall because of the greater penetration of wind into the canopy. The drag coefficient is therefore dynamic and cannot be represented by a single value as is normally the case with a rigid body. Typical values are given in Table 2.12.

Contrary to the above, the bulk drag coefficient has been found by Randall (1969) in apple orchards and Bache (1986) with cotton canopies to increase with increasing wind speed. This may be explained by the dependence of the above on the assumption that the whole leaf area contributes to the momentum transfer whereas, in reality, the effective foliage area for momentum absorption changes in a complex manner through streamlining, leaf flutter and plant vibration as the wind speed alters. In such cases, the terms *CD, z_0* and *d,* which express the effect of the vegetation in bulk, are only broad and not necessarily truthful indicators of what is happening. Also, their emphasis on conditions at the interface between the plant canopy and the atmosphere above, rather than on the soil surface beneath the vegetation, limits their value for determining the likelihood of wind erosion occurring.

An alternative and arguably more meaningful approach is to derive a drag coefficient *(Cd)* to describe the effect of the vegetation on the air within the plant layer. This is achieved by balancing the drag force of the wind profile exerted on the vegetation at height *(h)* with the extraction of momentum due to the frictional surface area of the individual foliage elements. This gives (Wright and Brown, 1967):

$$\tau(h) = 0.5\int_0^h Cd\,A(z)\,u(z)^2 dz, \tag{2.47}$$

where *A(z)* is the leaf area density (i.e. leaf area per unit volume).

Substituting equation 2.44 and rearranging yields:

$$Cd = 2u^{*2} \Big/ \int_0^h u^2 A(z) dz. \tag{2.48}$$

Wright and Brown (1967) found that values of *Cd* for maize leaves varied with height within the canopy and increased with increasing wind velocity. These results emphasize the importance of variations in vegetation structure and effective foliage area in controlling the amount of drag and, thereby, the form of the wind profile.

Figure 2.16 shows how wind velocity changes with height within the vegetative layer for a range of vegetation or crop types as a function of leaf area density (Landsberg and James, 1971). Equation 2.43 is only valid as an expression of the velocity profile in the air above the zero plane displacement. Below this, the wind profile may be fitted by one of the following equations:

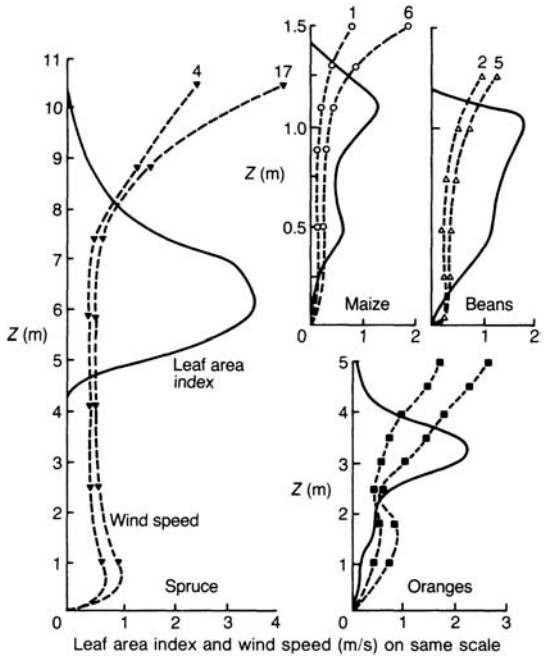

Figure 2.16 Wind velocity as a function of height and leaf area index for four crop types (after Landsberg and James, 1971). Two profiles are shown for each crop.

$$u(z) = u(h)\,(1 + m(1 - z/h))^{-2} \tag{2.49}$$

$$u(z) = u(h)\exp(-n(1 - z/h)), \tag{2.50}$$

where m is an experimental parameter which is characteristic of the vegetation type (Thom, 1971) and n is an attenuation coefficient which typically varies between 2 and 5 in value depending upon the foliage density and the type of vegetation (Inoue, 1963; Cionco, 1965).

Equations 2.49 and 2.50 are normally valid with tall vegetation such as trees. With shorter vegetation, for example, maize and rice, equation 2.50 describes the wind profile in the top half of the plant layer reasonably well but in the lower 20% of the profile the wind speeds decrease more slowly than the equation predicts (Denmead, 1976). Indeed, they may even increase close to the ground surface because of the sparser vegetation cover at the bottom of the plant layer. Wind tunnel studies (Morgan, Finney and Williams, 1986) on crops less than 0.15 m tall showed that the wind profile within the vegetation layer was better described by the equation:

$$u(z)/u(h) = 0.9 + 0.1\ln(z/h). \tag{2.51}$$

Shaw and Pereira (1982) and Hagen and Lyles (1988) also apply a log height-velocity relationship to the air in the lowest part of a vegetation cover close to the ground surface.

Morgan and Finney (1987) attempted to examine conditions in the lower part of the atmosphere by using equation 2.48 to calculate drag coefficients for the vegetation in the lowest 5 cm of single crop rows from field measurements of average 10 s wind velocities made with cup anemometers. They found that the drag coefficients both increased and decreased in value with wind speed (Figure 2.17), depending upon the consistency of the wind. If the latter is expressed by an index of turbulence *(TU),* defined as the ratio of the values of the standard deviation to the mean of a series of consecutive wind velocity recordings, the drag

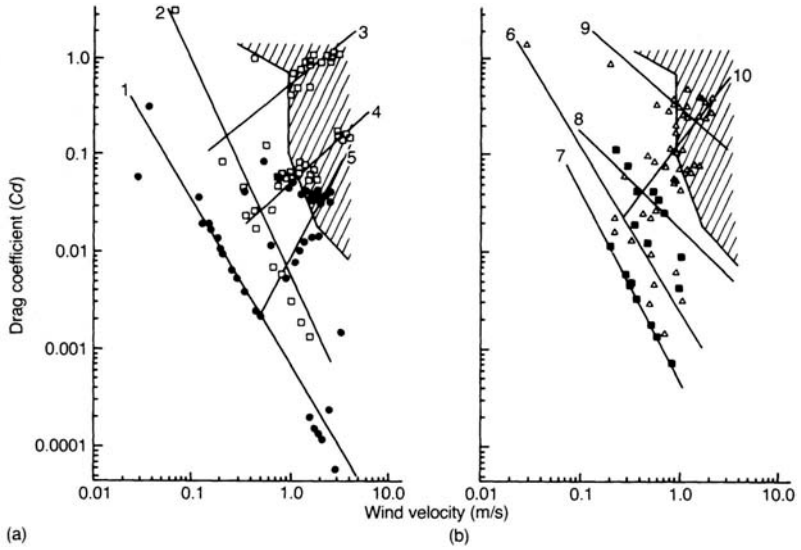

Figure 2.17 Relationships between drag coefficients *(Cd)* for the 5 cm layer of vegetation close to the ground surface and wind velocity measured at 5 cm height for (a) planted straw strips (●) and onions (□); and (b) live barley strips (■) and sugar beet (Δ). Shaded area represents risk of soil particle movement (from Morgan, 1989.)

coefficient decreases with increasing wind speed when $TU > 0.2$. For $TU \leqslant 0.2$, the drag coefficient increases with wind speed, presumably as a result of leaf flutter in the more continuous wind disturbing the atmosphere surrounding the foliage and setting up a 'wall' effect.

Although the correlation coefficient *(r)* between values of the drag coefficient and wind speed was always higher than –0.80 ($P<0.02$) for the negative relationship, it was generally lower for the positive one. This implies that wind speed alone does not adequately explain the variability in drag coefficients. Further insight is provided by wind tunnel studies (Morgan, Finney and Williams, 1988) of the drag coefficient of individual leaves *(CL)* as a function of their morphological properties of size, shape, fragmentation, orientation and rigidity. These showed that the single-leaf drag coefficient increased as the projected area and the deflection angle decreased and the down wind alignment increased. The results imply that highest drag is associated with greatest contact length between the wind and the air flow in a downwind direction and not with the area of foliage facing the wind; a finding which points to the importance of flow separation around the leaf and skin friction from the leaf surface over form drag in contributing to wind resistance. Since bladed leaves were found to have lower deflection angles than round or ovate leaves, it follows that high drag is associated with bladed leaves aligned downwind not as a result of streamlining but because of their natural growth position.

Information on foliage properties can add substantially to the understanding of drag coefficient *(Cd)* values in the lowest 5 cm of the atmosphere. From the field data of Morgan and Finney (1987), two relationships are obtained:

$$\log Cd = -1.648 - 1.406 \log u - 378.4\, PA + 0.00466\, H + 0.01045\, V \quad \text{for } TU > 0.2 \qquad (2.52)$$

$$(R = 0.839;\ n = 159),$$

$$\log Cd = -0.139 + 0.316 \log u - 369.1\, PA + 0.1167\, BM - 1.757\, TU \quad \text{for } TU \leqslant 0.2 \quad (R = 0.727;\ n = 130), \tag{2.53}$$

where u=wind velocity (m/s) at 5 cm height; PA=projected area of the foliage facing the wind (m^2); H=average angle of the leaves from the vertical in a downwind direction (degrees); V=average angle of the leaves from the vertical in a crosswind direction (degrees); BM=biomass (kg DM/m^3); and TU=turbulence index (described above).

The terms *PA, H, V* and *BM* are determined for a representative 10 cm length of a plant row in the lowest 5 cm of the atmosphere. Both equations show that the drag coefficient increases as the projected foliage area facing the wind decreases, again demonstrating the importance of contact length downwind between the leaf surfaces and the air. This is also implicit in the positive effects of downwind leaf alignment and increasing biomass, the latter being another indication of greater surface area of foliage. Typical values for *Cd* are given in Table 2.12.

This analysis shows that plant properties can have an important influence over values of the drag coefficient *(Cd)*. This, in turn, as combining equations 2.48 and 2.43 shows, has an effect on shear velocity:

$$u^* = 0.71 \int_0^h (CdA(z)\, u(z)\, dz)^{0.5}. \tag{2.54}$$

2.4 MECHANICAL EFFECTS

2.4.1 SOIL REINFORCEMENT

The roots and rhizomes of the vegetation interact with the soil to produce a composite material in which the roots are fibres of relatively high tensile strength and adhesion embedded in a matrix of lower tensile strength. The shear strength of the soil is therefore enhanced by the root matrix.

Field studies of forested slopes (O'Loughlin, 1984) indicate that it is the fine roots, 1–20 mm in diameter, that contribute most to soil reinforcement and that the larger roots play no significant role. Grasses, legumes and small shrubs can have a significant reinforcing effect down to depths of 0.75–1.5 m. Trees have deeper-seated effects and can enhance soil strength to depths of 3 m or more depending upon the root morphology of the species (Figure 2.18; Yen, 1972). Root systems lead to an increase in soil strength through an increase in cohesion brought about by their binding action in the fibre/soil composite and adhesion of the soil particles to the roots. It is generally held that roots have no effect on soil friction angle but Tengbeh (1989) found that grass roots increased the angle of internal friction of a sandy soil but had no such effect on a sandy clay loam.

The pattern of the relationship between soil cohesion and the roots is not known. Tengbeh (1989) found that Loretta grass *(Lolium perenne)* increased the cohesion (*c;* kPa) of soil as a function of root density (*RD;* Mg/m^3) in an exponential relationship so that for a sandy clay loam soil:

$$c = 10.54 + 8.63 \log RD \qquad r = 0.99,\ n = 16 \tag{2.55}$$

and for a clay soil:

$$c = 11.14 + 9.9 \log RD \qquad r = 0.99,\ n = 11. \tag{2.56}$$

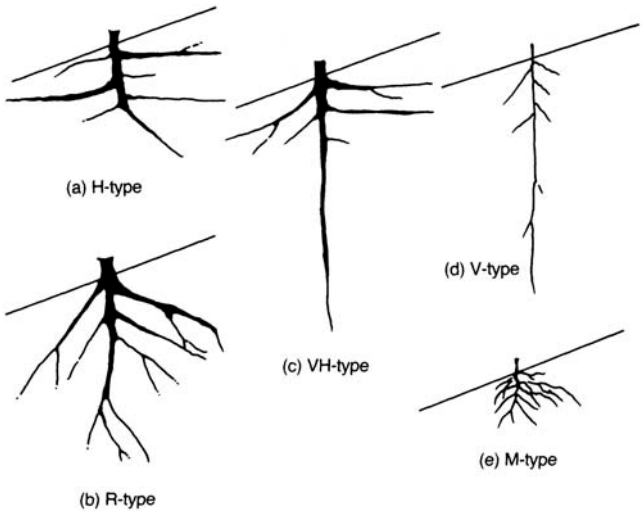

Figure 2.18 Patterns of root growth in trees (after Yen, 1987). (a) H-type: maximum root development occurs at moderate depth, with more than 80% of the root matrix found in the top 60 cm; most of the roots extend horizontally and their lateral extent is wide, (b) R-type: maximum root development is deep, with only 20% of the root matrix found in the top 60 cm; most of the main roots extend obliquely or at right angles to the slope and their lateral extent is wide, (c) VH-type: maximum root development is moderate to deep but 80% of the root matrix occurs within the top 60 cm; there is a strong tap root but the lateral roots grow horizontally and profusely, and their lateral extent is wide, (d) V-type: maximum root development is moderate to deep; there is a strong tap root but the lateral roots are sparse and narrow in extent, (e) M-type: maximum root development is deep but 80% of the root matrix occurs within the top 30 cm; the main roots grow profusely and massively under the stump and have a narrow lateral extent. H- and VH-types are considered beneficial for slope stabilization and wind resistance. H- and M-types are beneficial for soil reinforcement. The V-type is wind resistant.

In contrast, linear relationships have been obtained by Waldron (1977) between the change in soil shear strength and the root area ratio of barley roots in a silty clay loam soil, and by Ziemer (1981) between shear strength and root biomass of *Pinus cordata* in a sand.

These studies show that root reinforcement can make significant contributions to soil strength, even at low root densities and low shear strengths. Equations 2.55 and 2.56 indicate that cohesion increases rapidly with increasing root density at low root densities but that increasing root density above 0.5 Mg/m^3 on the clay soil and 0.7 Mg/m^3 on the sandy clay loam soil has little additional effect. This implies that vegetation can have its greatest effect close to the soil surface where the root density is generally highest and the soil is otherwise weakest.

Since shear strength affects the resistance of the soil to detachment by raindrop impact (Cruse and Larson, 1977; Al-Durrah and Bradford, 1982), and the susceptibility of the soil to rill erosion (Laflen, 1987; Rauws and Govers, 1988) as well as the likelihood of mass soil failure, root systems can have a considerable influence on all these processes. The maximum effect on resistance to soil failure occurs when the tensile strength of the roots is fully mobilized and that, under strain, the behaviour of the roots and the soil are compatible. This requires roots of high stiffness or tensile modulus to mobilize sufficient strength and the 8–10% failure strains of most soils. The tensile effect is limited with shallow-rooted vegetation where the roots fail by pullout, i.e. slipping due to loss of bonding between the root and the soil, before peak tensile strength is reached (Waldron and Dakessian, 1981). The tensile effect is most marked with trees where the

roots penetrate several metres into the soil and their tortuous paths around stones and other roots provide good anchorage. Root failure may still occur, however, by rupture, i.e. breaking of the roots when their tensile strength is exceeded. The strengthening effect of the roots will also be minimized in situations where the soil is held in compression instead of tension, e.g. at the bottom of hillslopes. Root failure here occurs by buckling.

2.4.2 ROLE OF ORGANIC MATTER

The return of vegetative material to the soil as organic matter plays a vital role in aggregation of the soil particles. Aggregate-stabilizing compounds are formed during the degradation of organic material, such as manure, plant roots, leaves and stems, and straw, by microbial and faunal activity within the soil. Thus, the level of biological activity or the speed of degradation of organic matter are probably better indicators of the relative stability of soil aggregates than the content of organic matter as such. A good vegetative cover is likely to increase the biological activity and the rate of aggregate formation, but no quantification of this effect can be given. Increased aggregate stability of a soil increases permeability and infiltration which, in turn, reduces surface runoff and enhances the available water content for plant growth. This promotes better vegetation growth with greater protection of the soil surface and a drier soil environment.

The size and stability of the soil aggregates affects their detachability by raindrop impact and their detachability and transportability by surface runoff. Several of the transport equations (section 2.3.2) contain factors of the type d^{-x}, where x varies between 1.0 and 1.54, showing that transport capacity becomes inversely related to the diameter of the aggregates. As the Engelund-Hansen sediment transport relationship (equation 2.21) indicates, transportability is also dependent on the density of the soil particles. Thus, large soil aggregates are moved before primary particles of the same diameter because their densities are approximately 1.8–2.0 Mg/m^3 compared with 2.6 Mg/m^3 for sand.

2.4.3 ROOT WEDGING

Root wedging is a potentially destabilizing process whereby fissures and joints in rocks are opened up by the advance and growth of roots. Trees create the biggest problem, though grass roots can also force open small cracks. Where vegetation gains a hold on steep slopes with steeply-inclined joint planes or fissures, the wedging action of plant roots can dislodge and topple blocks or sections of the rock. Earth (soil) slopes are less likely to be affected.

Root wedging may not cause instability during the lifetime of a tree as the rocks may be enveloped within the roots and trunk. It is on the death of the tree that dislodged blocks are likely to fall free.

2.4.4 ARCHING AND BUTTRESSING

The tap and sinker roots of many tree species extend through the soil layers and into the underlying bedrock, anchoring them to the slope. The trunks and large roots then act in the same way as stabilizing piles and buttress the soil, restraining it from movement down-slope. The extent to which buttressing can contribute to the stability of the soil mass on a slope depends upon the depth of the soil mantle and the

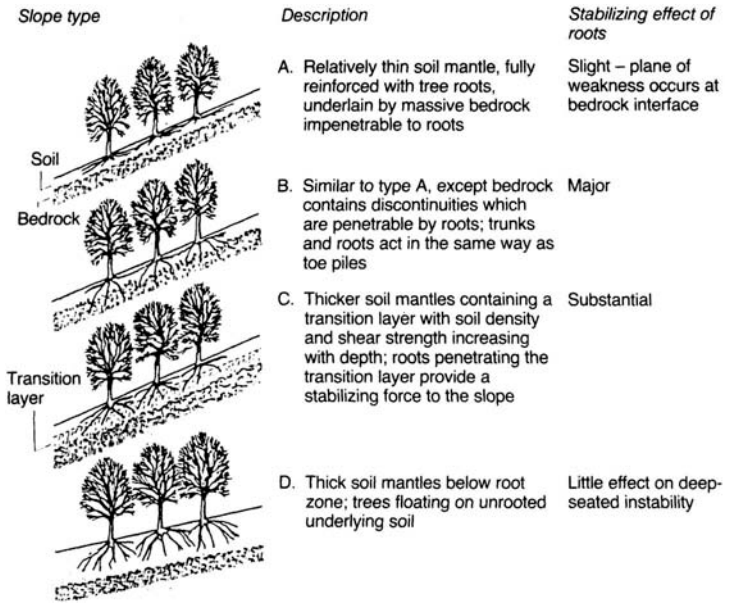
Slope type
Description
Stabilizing effect of roots
Soil
Bedrock
Transition layer
A. Relatively thin soil mantle, fully reinforced with tree roots, underlain by massive bedrock impenetrable to roots
Slight – plane of weakness occurs at bedrock interface
B. Similar to type A, except bedrock contains discontinuities which are penetrable by roots; trunks and roots act in the same way as toe piles
Major
C. Thicker soil mantles containing a transition layer with soil density and shear strength increasing with depth; roots penetrating the transition layer provide a stabilizing force to the slope
Substantial
D. Thick soil mantles below root zone; trees floating on unrooted underlying soil
Little effect on deep-seated instability

Figure 2.19 Classes of plant-root reinforced and anchored slopes (after Tsukamoto and Kusakabe, 1984).

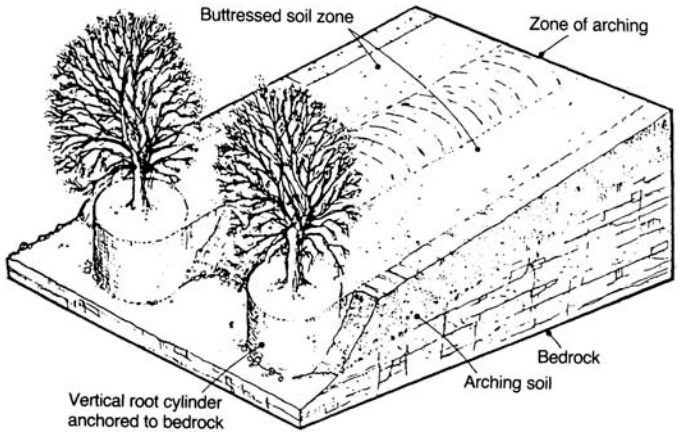

Figure 2.20 Schematic representation of soil buttressing and arching (after Wang and Yen, 1974).

groundwater as well as on the penetrability of the bedrock by roots (Figure 2.19; Tsukamoto and Kusakabe, 1984).

Where trees are sufficiently close together, the soil between the unbuttressed parts of the slope may gain strength by arching (Figure 2.20). Based on work by Wang and Yen (1974), Gray (1978) has produced a plot of the theoretical critical (minimum) spacing required for arching to occur on a 40° slope with a 0.9 m deep sandy soil mantle (Figure 2.21). This shows that the critical spacing depends upon the cohesiveness of the underside of the supported soil mass. If cohesion is zero and the residual friction along the underside is half the peak friction, the critical spacing is only 1.2 m. If a cohesion of 2.4 kN/m^2 is assumed, with a

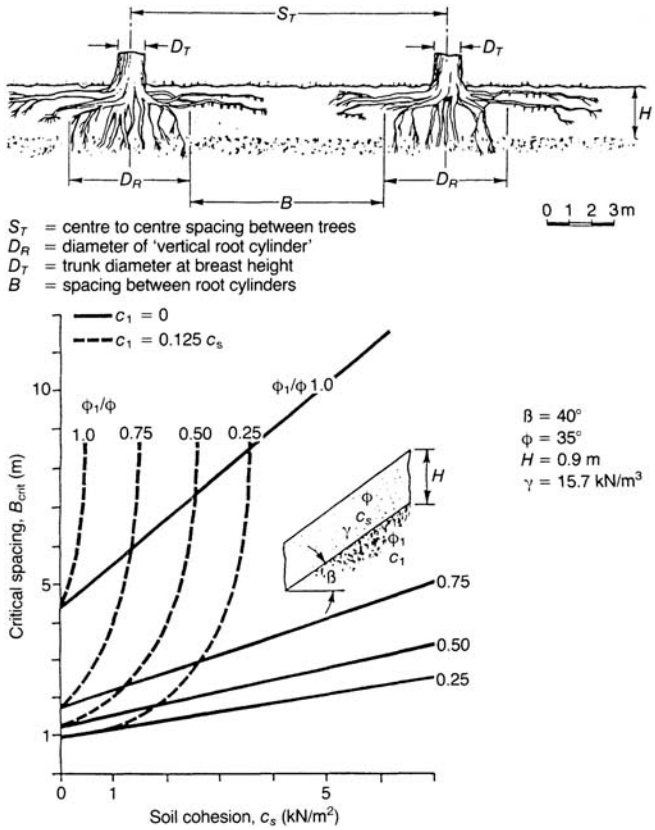

Figure 2.21 Critical spacing of trees for arching based on the theory of Wang and Yen (1974) applied to a steep sandy slope (after Gray and Leiser, 1982).

residual cohesion of 12.5% of this value, the critical spacing increases to 6.4 m. Tree spacings on such slopes in the field are often of the right order for arching to develop.

2.4.5 SURCHARGING

Surcharge arises from the additional weight of the vegetation cover on the soil. This effect is normally considered only for trees, since the weight of grasses and most herbs and shrubs is comparatively small. Surcharge increases the downslope forces on a slope, lowering the resistance of the soil mass to sliding, but it also increases the frictional resistance of the soil. Bishop and Stevens (1964) show that large trees can increase the normal stress on a slope by up to 5 kN/m^2 but that no more than half contributes to an increase in shear stress. Generally, the second effect outweighs the first, so that, overall, surcharge is beneficial. Nevertheless, surcharge at the top of a slope can reduce overall stability whereas, at the bottom of the slope, it will increase stability.

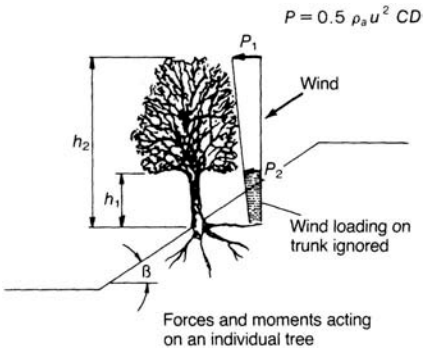

Figure 2.22 Effect of wind loading on a single tree (from Coppin and Richards, 1990).

De Ploey (1981) invokes surcharge combined with lowering of the cohesion of the soil mass through increased infiltration and, therefore, increased soil water content, as contributing to landslides on the forested slopes of the Serra do Mar, east of Santos, in Brazil. The surcharge becomes critical when rainfall of several hundreds of millimetres occurs in a wet spell of a few days; for example, on 17 and 18 March 1967 when daily rainfalls totalled 260 and 420 mm respectively. In such events, interception and evapotranspiration are reduced virtually to zero and the soil is unable to either dry out or drain. The critical factors here may well be the low angle of internal friction of the soil material which, when close to waterlogging, is reduced to less than 20°, and the steepness of the slopes, which are over 20°. In contrast, Gray and Megahan (1981) state that surcharge is beneficial when cohesion is low and groundwater levels are high provided that the angle of internal friction of the soil is also high and the slope angles are low.

2.4.6 WIND LOADING

The pressure *(P)* exerted on a vegetation cover by wind can be transmitted to the soil as an increased loading *(D),* reducing its resistance to failure. From the work of Hsi and Nath (1970) and Brown and Sheu (1975), for a single tree (Figure 2.22):

$$D = \sum_{i=h1}^{i=h2} (0.5\rho_a u^2 CD \cos^2 \beta b) i, \tag{2.57}$$

where D=drag force (kg) transmitted into the slope; $h1$=height of the bottom of the tree canopy above the ground (m); $h2$=height of the top of the tree canopy above the ground; ρ_a=density of the air (kg m^3); u=wind velocity (m/s); CD=the bulk drag coefficient of the vegetation; β=slope angle (degrees); and b=transverse width of the crown (m) at each height increment, i.

Wind loading is only significant for trees and when the wind velocity exceeds 11 m/s.

Wind pressure on a tree can also produce a destabilizing moment which, if the tree is not well anchored, will cause it to topple over. Increased infiltration of water into the soil through the scar created by the uprooted tree can then lower the resistance of the whole soil mass to failure.

2.4.7
SURFACE PROTECTION

Vegetation protects the soil mechanically by absorbing directly the impact of walkers, livestock and vehicles. Most studies of this effect have concentrated on the resistance of vegetation to damage by walking. When an individual walks over the ground surface, the soil and vegetation are compacted in the early part of each step under the pressure of the heel; at the end of the step, they are sheared by the movement of the toe. The shearing action is the most damaging (Quinn, Morgan and Smith, 1980).

Broadly, grasses are reasonably resistant and can withstand between 1000 and 2000 passes by walkers before the density of cover falls below 50%. In contrast, alpine plant communities can withstand about 60 passes and arctic tundra communities only eight passes (Liddle, 1973).

The effect of walking on shrubs is greater than that on grasses because plants that produce buds and shoots at or below ground level have their growth points protected by the overlying foliage as the vegetation is flattened underfoot. They are therefore less easily damaged. For this reason, heath and bracken disappear more rapidly than grasses in upland areas under heavy recreational use.

2.5
VISUALIZATION

In order to visualize the combined effect when several vegetation-related parameters are varied simultaneously, some simple calculations are presented. The numerical values should not be taken too seriously, as the overall results only illustrate the theoretical principles previously discussed. Nevertheless, the influence of vegetation is demonstrated to about the right order of magnitude.

2.5.1
WATER EROSION

The effect of vegetation cover on water erosion is illustrated for seven conditions for which typical values of percentage cover and plant height are presented in Table 2.13. A value of saturated hydraulic conductivity has been chosen for a loamy soil and then varied, on the basis of McKeague, Wang and Coen (1986), taking account of the number of biopores and the level of soil aggregation expected under each condition. Values of Manning's *n* are selected from Engman (1986). The soil is assumed wet, so the infiltration rate is regarded as equal to the saturated hydraulic conductivity.

The accumulated runoff water is calculated for four rainfall intensities, three slope lengths or distances downslope, and two slope steepnesses. For each combination, the water depth, flow velocity and, using the Engelund and Hansen (1967) formula, transport capacity relative to that on bare soil are determined. Soil detachment by raindrop impact is calculated relative to that for bare soil using the procedure of Styczen and Høgh-Schmidt (1988). None of the calculations take into consideration an

Table 2.13 Parameters used for assessment of the effect of vegetation on erosion by water

Cover type	*Saturated hydraulic conductivity (mm/h)*	*Manning's* n	*Percentage cover*	*Height (m)*
Bare soil	10	0.01	0	
Grass	50	0.20	90	0
Soya beans	25	0.04	80	0.5

Cover type	*Saturated hydraulic conductivity (mm/h)*	*Manning's* n	*Percentage cover*	*Height (m)*
Maize	25	0.02	80	1.5
Agricultural crops and crusted soil	5	0.02	80	1.5
Eucalyptus and crusted soil	5	0.01	80	3–8
Eucalyptus with grass	50	0.20	80–90	3–8/0

aggregate size distribution of the soil. A crusting index (Table 2.14) is developed based on the

Table 2.14 Crusting index calculated as a function of rainfall energy. The index unit is the energy received relative to that on a bare soil when the rainfall intensity is 25 mm/h

	Rainfall intensity (mm/h)			
Cover	*25*	*50*	*75*	*100*
Bare soil	1	2.2	3.6	5.0
Grass, 90% cover	0.1	0.2	0.4	0.5
Soya beans	0.5	1.0	1.5	2.1
Maize	1.1	2.0	3.2	4.3
Eucalyptus, crusted soil	2.8	5.4	7.9	10.4
Eucalyptus with grass	0.3	0.5	0.8	1.0

energy of the rainfall received at the ground relative to that received by a rain of 25 mm/h intensity on a bare soil. A rilling index (Table 2.15) is calculated as the product of runoff volume, slope length and slope steepness.

In Figure 2.23, curves representing relative transport capacities and soil detachment by raindrop impact are presented for each condition. According to the value chosen for soil erodibility, the curves for soil detachment may be multiplied by a constant and the cross-over points of the two curves will change accordingly. Detachment by runoff has not been added as its relative importance depends upon erodibility. It is, however, probably proportional to the transport capacity. The curves for soil detachment differ from those presented in a similar

Table 2.15 Rilling index calculated as the product of runoff, slope length and slope steepness for a 5% slope and different rainfall intensities

	Rainfall intensity (mm/h)			
Cover type	*25*	*50*	*75*	*100*
Slope length 20 m				
Bare soil	0.15	0.4	0.65	0.9
Grass	0	0	0.25	0.5
Soya beans	0	0.25	0.5	0.5
Maize	0	0.25	0.5	0.75
Agricultural crops with crusted soil	0.2	0.45	0.7	0.95
Eucalyptus with crusted soil	0.2	0.45	0.7	0.95
Eucalyptus with grass	0	0	0.25	0.5

	Rainfall intensity (mm/h)			
Cover type	*25*	*50*	*75*	*100*
Slope length 50 m				
Bare soil	0.38	1.0	1.63	2.25
Grass	0	0	0.63	1.25
Soya beans	0	0.63	1.25	1.88
Maize	0	0.63	1.25	1.88
Agricultural crops with crusted soil	0.5	1.13	1.75	2.38
Eucalyptus with crusted soil	1.0	1.13	1.75	2.38
Eucalyptus with grass	0	0	0.63	1.25
Slope length 100 m				
Bare soil	0.75	2.0	3.25	4.5
Grass	0	0	1.25	2.5
Soya beans	0	1.25	2.5	3.75
Maize	0	1.25	2.5	3.75
Agricultural crops with crusted soil	1.0	2.25	3.5	4.75
Eucalyptus with crusted soil	1.0	2.25	3.5	4.75
Eucalyptus with grass	0	0	1.25	2.5

exercise by Foster and Meyer (1975) because the procedure used here relates the splashed material transported away to the quantity of the runoff instead of assuming that all the splashed particles are available for transport.

At the top of the slope (represented by the 20 m slope length), where only small amounts of runoff occur, the erosion is transport-limited except under grass. Further downslope (50 m slope length), where more runoff accumulates, the transport capacity exceeds soil detachment and the erosion becomes detachment-limited for conditions with vegetation close to the surface and for bare soil. At the foot of the slope, after 100 m slope length, erosion is detachment-limited except for trees without undergrowth and litter. However, even though erosion remains transport-limited under trees, the large amounts of runoff water accumulated may cause rilling to occur. In this case, detachment in the rills may dominate the erosion completely. As the transport capacity and the erosive capacity of rill flow are much larger than for sheet flow, much more material can be expected to be **Figure 2.23** (cont.) removed from an area when rills form. Passing the threshold for rill formation means a serious acceleration in water erosion.

A major difference between the curves is the starting point at which runoff commences. This hydrological effect may be just as important in determining the magnitude of erosion as the effects of vegetation on runoff volume.

The difference in the transport capacity for maize and soya bean is due to differences in surface roughness, while the difference in soil detachment by raindrop impact is due to the different plant heights. The curves for grass show a very low amount of runoff generated, a high degree of roughness and almost no detachment.

The most serious condition is for the trees without cover. This is because of the large amounts of runoff which are generated very quickly after the onset of the storm, due to high values of the crusting index, and the high flow velocities. Despite the large amounts of runoff, soil loss is transport-limited, indicating extremely

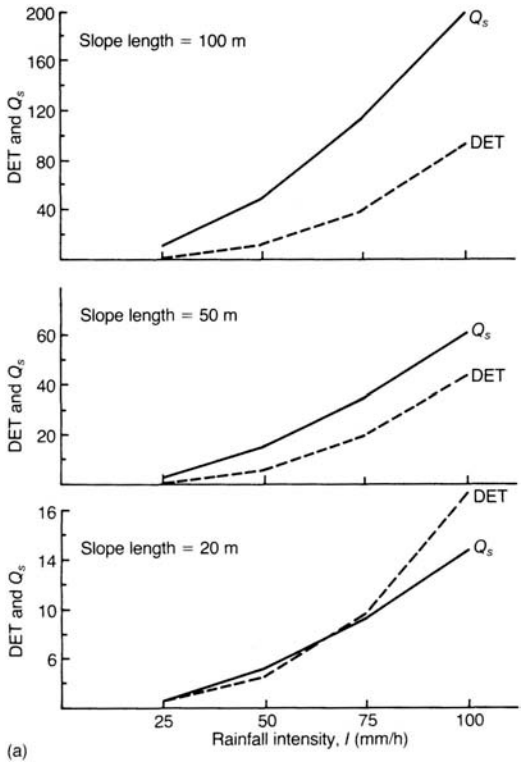

Figure 2.23 Relative transport capacities (Q_s) and soil detachment (DET) by splash as a function of rainfall intensity on a 5% slope for slope lengths of 100 m, 50 m and 20 m on (a) bare soil; (b) grass with and without a cover of Eucalyptus; (c) soya beans; (d) maize; (e) soya beans and maize on a crusted soil; and (f) bare soil with and without a crust under Eucalyptus. Note that the scales of the *y*-axis differ for the three slope lengths.

high detachment rates which arise from the high fall heights of the leaf drainage. The rilling index is larger here than in any of the other cases.

Two studies which support the validity of the last case have been carried out in Java, Indonesia, by Coster (1938) and Wiersum (1985). Both authors studied the effects of various vegetation layers in an *Acacia auriculiformis* forest on surface erosion by removing **Figure 2.23** (cont.) one vegetation layer at a time. Their findings clearly illustrate the importance of the height of the canopy above the soil surface and the importance of a ground vegetation or litter cover.

Coster (1938; Table 2.16) found that far more erosion occurred under trees without undergrowth and litter than on bare soil. When the trees were removed but litter and undergrowth kept intact, the soil loss was only 1/15th of that from bare soil. In the undisturbed forest, the soil loss was very low. Wiersum (1985) obtained less drastic differences but at least 20 times as much soil was lost when litter was removed compared to when litter was present. When both litter and undergrowth are intact, hardly any erosion occurs.

In both cases, it is the vegetation close to the soil surface and the litter that play the important role in controlling the erosion. Although the vegetation layers in the canopy catch rainwater and divert some to stemflow, these effects are more than offset by the increase in drop size of the rain which reaches the ground surface as leaf drainage.

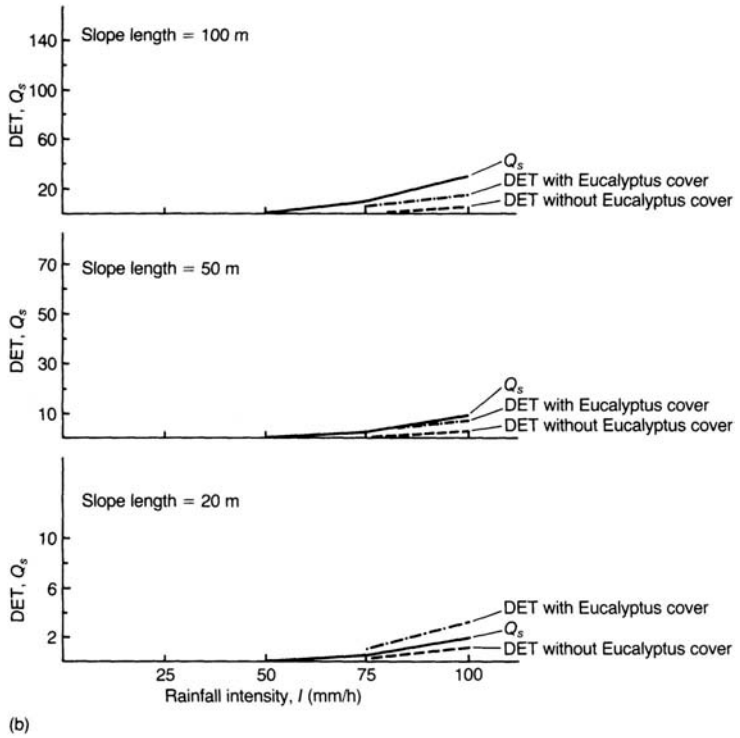

2.5.2 SLOPE STABILITY

The stability of a slope against failure is evaluated by the factor of safety *(F),* which is defined as the ratio of the resistance of the soil mass to shear along a potential slip plane to the shear force acting on that plane. Soil failure occurs when the ratio falls to unity. The simple case of a translational failure along a sliding surface **Figure 2.23** (cont.) parallel to the ground over a relatively long uniform slope can be analysed by infinite slope analysis. In this case, a single element or segment (Figure 2.24) of the slope can be considered as representative of the whole, and the head and toe portions of the slope are ignored as being negligible in extent.

Using effective stress analysis, the factor of safety without vegetation can be defined by:

$$F = \frac{c' + (\gamma z - \gamma_w h_w)\cos^2\beta \tan\phi'}{\gamma z \sin\beta \cos\beta}, \tag{2.58}$$

where c'=effective soil cohesion (kN/m^3); γ=unit weight of soil (kN/m^3); z=vertical height of soil above the slip plane (m); β=slope angle (degrees); γ_w=unit weight of water (=9.8 kN/m^3); h_w=vertical height of groundwater table above the slip plane (m); and ϕ'=effective angle of internal friction of the soil material (degrees).

Figure 2.25, based on Coppin and Richards (1990), shows the main influences of vegetation on the stability of the slope segment. They can be included in the calculations of the factor of safety as follows:

$$F = \frac{(c' + c'_R) + \{[(\gamma z - \gamma_w h_w) + W]\cos^2\beta + T\sin\theta\}\tan\phi' + T\cos\theta}{[(\gamma z + W)\sin\beta + D]\cos\beta}, \tag{2.59}$$

Figure 2.23 (cont.)

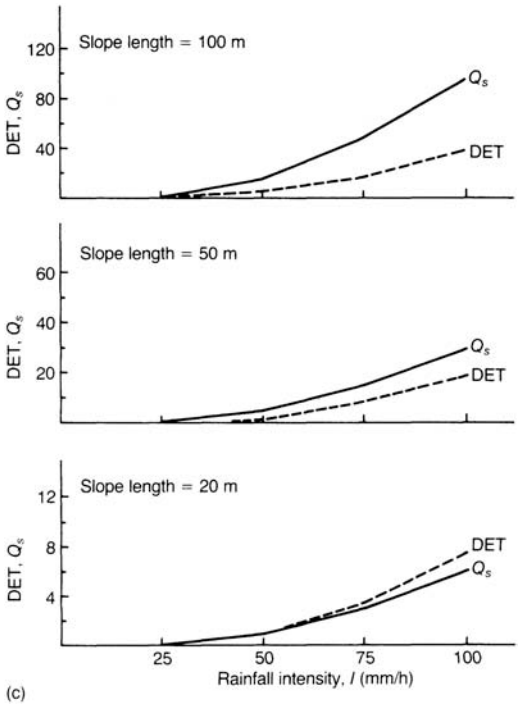

(c)

where c'_R=enhanced effective soil cohesion due to soil reinforcement by roots (kN/m^3); W=surcharge due to weight of the vegetation (kN/m^2); h_v=vertical height of groundwater table above the slip plane with the vegetation (m); T=tensile root force acting at the base of the slip plane (kN/m); θ=angle between roots and slip plane (degrees); and D=wind loading force parallel to the slope (kN/m).

Appendix 2.A gives the calculations for the factor of safety for a sample slope segment with and without vegetation. The calculations are purely illustrative but they show that the vegetation increases the factor of safety by 55%, assuming that the tensile strength of the roots is fully mobilized, and by 17%, if this effect (T acting over angle θ) is ignored. The greatest effects are due to the increase in cohesion through root reinforcement of the soil and to the tensile strength of the roots themselves across the potential slip surface. Although field studies of the effect of vegetation on slope stability are rare, Greenway (1987) found that the additional cohesion brought about by tree roots increased the factor of safety on wooded slopes in Hong Kong by 29%.

2.6
SALIENT PROPERTIES OF VEGETATION

The calculations presented in the previous section demonstrate that the overall effect of vegetation is the result of a balance between **Figure 2.23** (cont.)

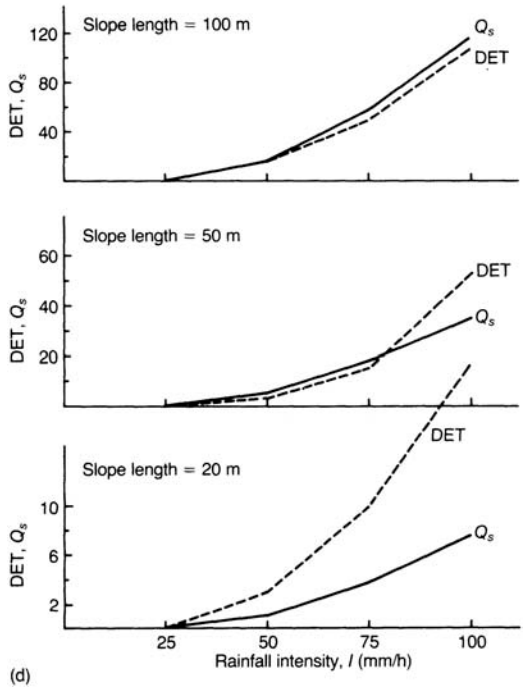

Table 2.16 Erosion (kg/m^2 y) in a montane forest, Java, Indonesia (after Wiersum, 1985 from table in Coster, 1938)

Cover	*Number of observations (plot years)*	*Measured erosion*	*Erosion adjusted for equivalent slope and rainfall*
Undisturbed forest	2	0.03	0.01
Trees removed	5	0.04	0.03
Undergrowth removed	4	0.06	0.05
Trees and undergrowth removed	1	0.08	0.02
Undergrowth and litter removed	10	4.32	2.61
Trees, undergrowth and litter removed	2	1.59	0.44
Shrub vegetation	4	0	0
Shrubs removed	3	0.20	0.23

beneficial and adverse influences. These have been summarized by Coppin and Richards (1990), as shown in Table 2.17. The nature of the balance and, therefore, the engineering function which individual plants perform will depend upon their structure or architecture. Plants with strong tap and sinker roots will help stabilize a slope through arching and buttressing, whereas plants with a dense lateral rooting system will increase the strength of the top layer of the soil by adding to cohesion. In contrast, surface erosion processes are more strongly influenced by the above-ground growth of the vegetation. The properties of the vegetation which influence its engineering function are listed in Table 2.18, also taken from Coppin and Richards (1990). Many of these properties vary with the stage of vegetation growth and therefore alter both

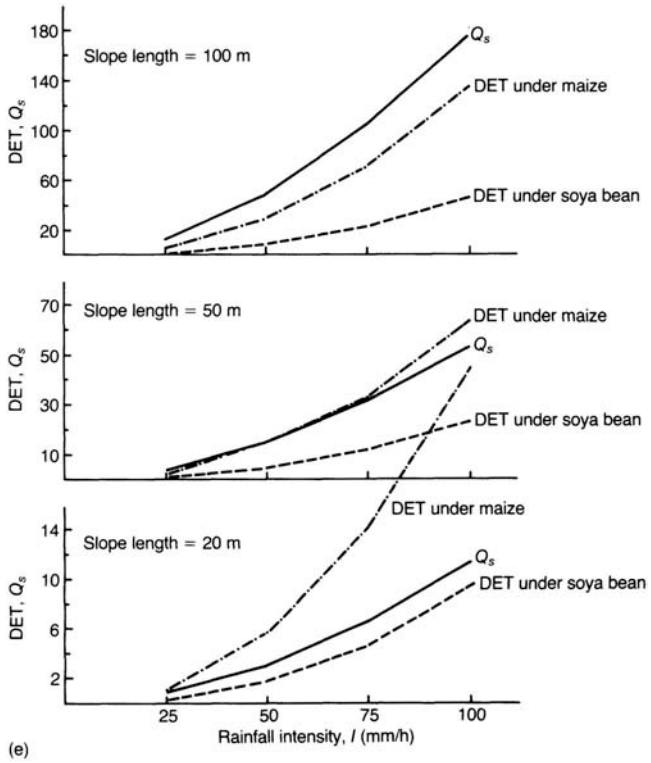

(e)

seasonally and, through ecological succession, over a longer time. Increasing cohesion of the soil through vegetation growth can offset long-term decreases in soil strength brought about by weathering and the fissuring and progressive softening of overconsolidated clays.

There is a close relationship between vegetation and erosion. On the one hand, vegetation, through its engineering functions, can control the amount of erosion which takes place. On the other hand, erosion can produce such a hostile and unstable environment that vegetation will not grow. The balance and competitiveness of the erosion-vegetation system has been analysed by Thornes (1988a,b, 1990) with respect to southeast Spain. He assumes that erosion limits plant growth through water and nutrient stress but that vegetation also limits erosion. Such an ecosystem may be in balance, or it may be self-reinforcing in one direction or another. For example, erosion will result in less vegetation which will produce a deteriorating water balance with less water available for plant growth and more water contributing to runoff and erosion. Alternatively, an increase in vegetation growth will lead to less erosion and a more favourable water balance for further vegetation. If grazing pressure is added to the ecosystem, a higher biomass production is necessary to keep the system in balance. Otherwise the situation may change from equilibrium to deterioration. The details of the system in southeast Spain are very complex because litter fall occurs at different times of year for different plant species and because a certain amount of the litter is removed by the runoff. One of the important effects of the ground vegetation is to keep the litter in place.

Most vegetation is self-regenerating but human and animal interference may destroy the natural cycles of plant growth. A good understanding of both natural and man-influenced ecosystems is therefore essential for analysing and predicting the engineering role of vegetation. Continuous hard grazing generally leads to loss of the vegetation cover; the plants lack sufficient leaves for photosynthesis and die, whilst damage to the

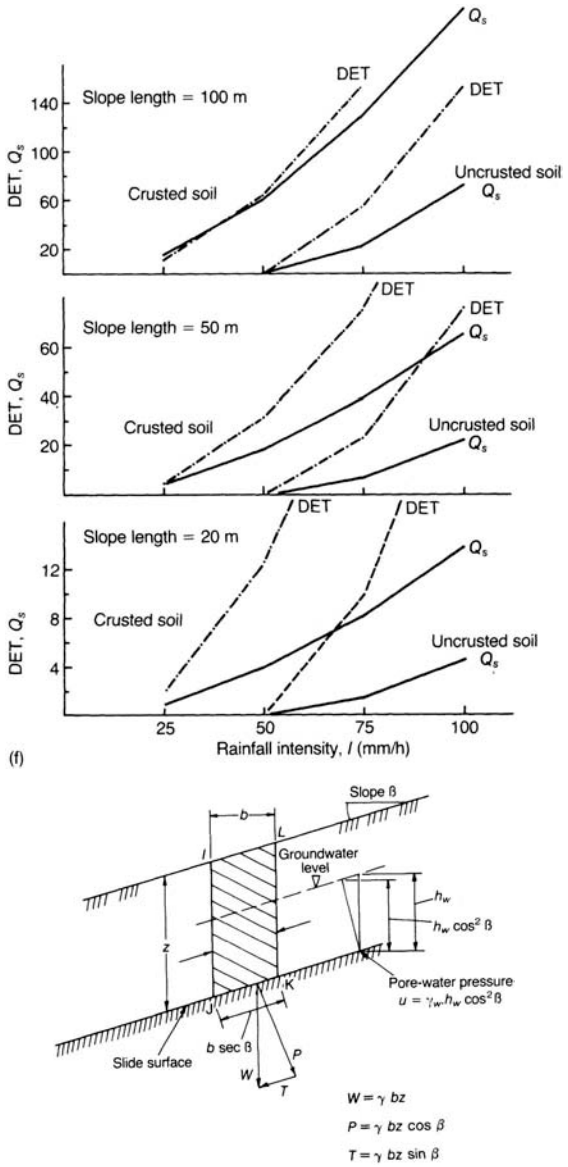

Figure 2.24 Factors involved in the infinite slope method for analysing slope stability (Notation in text.)

growth points prevents their regeneration. These relationships are analysed theoretically in THEPROM, an erosion-productivity model being developed for rangelands in Botswana (Biot, 1990). Under special circumstances, however, the interactions may react another way. Valentin (1985) showed that, under very special ecological conditions, grassland vegetation may be improved by cattle grazing.

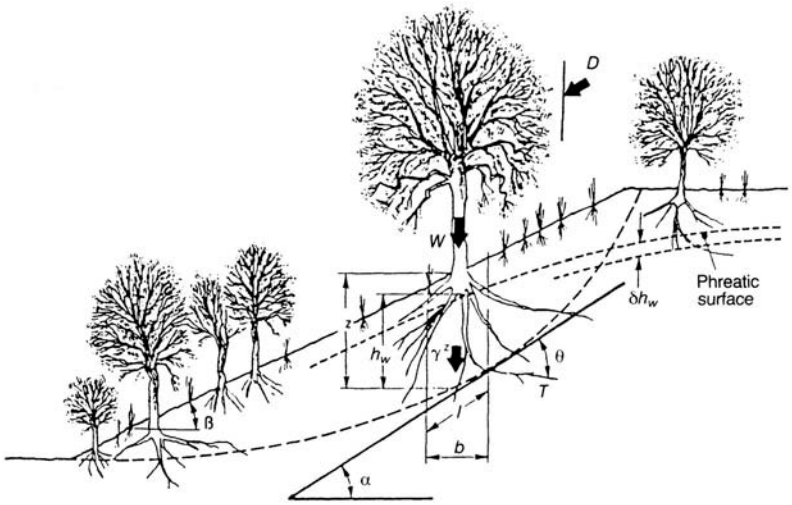

Figure 2.25 Main influences of vegetation on slope stability (after Coppin and Richards). Parameters applied in slope stability analysis:

	γ^z	Total weight of soil slice (kN/m^2)
	c', ϕ'	Effective strength parameters at slip surface
	l	Length of slip surface with slice, m (b sec α)
	u	Pore-water pressure at slip surface (kN/m^2) ($\gamma_w h_w$)
Due to vegetation	u_v	Decrease in pore-water pressure to evapotranspiration by vegetation at slip surface (kN/m^2) (2)
	c'_R	Enhanced effective soil cohesion due to root matrix reinforcement by vegetation along slip surface (kN/m^2)
	c'_S	Enhanced effective soil cohesion due to soil suction due to evapotranspiration by vegetation at slip surface (kN/m^2)(2)
	W	Surcharge due to weight of vegetation (kN/m)
	D	Wind loading force parallel to slope (kN/m)
	T	Tensile root force acting at base of slice (kN/m) (assumed angle between roots and slip surface, θ)
	z	Vertical height of surface of soil layer above slip plane (m)
	h_w	Vertical height of phreatic surface or water table above slip surface (m)

Notes

1. The value of many of these parameters varies with depth and soil type.

2. In certain slope stability analyses the decrease in pore-water pressure due to vegetation (i.e. increased soil suction from evapotranspiration) is expressed as an enhanced effective soil cohesion, as distinct from a pore pressure reduction.

Table 2.17 Beneficial and adverse effects of vegetation (from Coppin and Richards, 1990)

Hydrological effects		*Mechanical effects*	
Foliage intercepts rainfall causing:		Roots bind soil particles and permeate the soil, resulting in:	
1. absorptive and evaporative losses, reducing rainfall available for infiltration	B	1. restraint of soil movement reducing erodibility	B
2. reduction in kinetic energy of raindrops and thus erosivity	B	2. increase in shear strength through a matrix of tensile fibres	B

Hydrological effects		*Mechanical effects*	
3. increase in drop size through leaf drip, thus increasing localized rainfall intensity	A	3. network of surface fibres creates a tensile mat effect, restraining underlying strata	B
Stems and leaves interact with flow at the ground surface, resulting in:		Roots penetrate deep strata, giving:	
1. higher depression storage and higher volume of water for infiltration	A/B	1. anchorage into firm strata, bonding soil mantle to stable subsoil or bedrock	B
2. greater roughness on the flow of air and water, reducing its velocity, but	B	2. support to up-slope soil mantle through buttressing and arching	B
3. tussocky vegetation may give high localized drag, concentrating flow and increasing velocity	A	Tall growth of trees, so that:	
1. weight may surcharge the slope, increasing normal and down-slope force components	A/B		
Roots permeate the soil, leading to:		2. when exposed to wind, dynamic forces are transmitted into the ground	A
1. opening up of the surface and increasing infiltration	A		
2. extraction of moisture which is lost to the atmosphere in transpiration, lowering pore-water pressure and increasing soil suction, both increasing soil strength	B	Stems and leaves cover the ground surface, so that:	
1. impact of traffic is absorbed, protecting soil surface from damage	B		
3. accentuation of dessication cracks, resulting in higher infiltration	A	2. foliage is flattened in high velocity flows, covering the soil surface and providing protection against erosive flows	B

A=adverse effect
B=beneficial effect

APPENDIX 2.A:

Estimation of the effect of vegetation on the factor of safety on a slope using the infinite slope method. Notation is given in the text.

Table 2.18 Salient properties of vegetation and their engineering significance (from Coppin and Richards, 1990)

Vegetation		Vegetation properties										
Effect on	*Influence*	*Ground cover (%)*	*Height*	*Leaf shape and length*	*Stem/leaf density*	*Stem/leaf robustness*	*Stem/leaf flexibility*	*Root depth*	*Root density*	*Root strength*	*Annual growth cycle*	*Weight*
Surface competence												
	Soil detachment	●	●	●	●						●	
	Mechanical strength	●	●		●	●			●	●	●	
	Insulation	●			●						●	
	Retarding/arresting		●		●	●	●					
	Erosion	●			●						●	
Surface water regime												
	Rainfall interception	●		●	●							
	Overland flow/runoff	●			●							
	Infiltration				●			●	●			
	Subsurface drainage							●	●			
	Surface drag	●	●	●	●		●				●	
Soil water												
	Evapotranspiration			●	●				●		●	
	Soil moisture depletion leading to increased soil suction, reduced pore-water and soil weight							●			●	
Properties of soil mass												
	Root reinforcement							●	●	●	●	
	Anchorage/restraint							●	●	●		
	Arching/buttressing							●		●		
	Surface mat/net								●	●	●	
	Surcharge		●									●
	Windthrow		●		●	●		●		●	●	●
	Root wedging							●	●			
Air flow												
	Surface drag		●	●	●		●				●	
	Flow deflection		●		●	●	●				●	
	Noise attenuation		●	●	●						●	
	Suspended particulates		●		●						●	

FACTOR OF SAFETY WITHOUT VEGETATION:

$$F = \frac{c' + (\gamma z - \gamma_w h_w)\cos^2\beta \tan\phi'}{\gamma z \sin\beta \cos\beta}$$

$c' = 10\,\text{kN/m}^3$

$\gamma = 18\,\text{kN/m}^3$

$z = 1.0\,\text{m}$

$\beta = 35°$

$\phi' = 35°$

$\gamma_w = 9.8\,\text{kN/m}^3$

$h_w = 0.5\,\text{m}$

$$F = \frac{10 + \{(18 \times 1) - (9.8 \times 0.5)\} \times 0.6710 \times 0.7002}{18 \times 0.5736 \times 0.8192}$$

$$F = \frac{10 + \{18 - 4.9\} \times 0.6710 \times 0.7002}{8.4581}$$

$$F = \frac{16.1548}{8.4581}$$

$F = 1.91$

FACTOR OF SAFETY WITH VEGETATION

$$F = \frac{(c' + c'_R) + [\{(\gamma z - \gamma_w h_v) + W\}\cos^2\beta + T\sin\theta]\tan\phi' + T\cos\theta}{\{(\gamma z + W)\sin\beta + D\}\cos\beta}$$

$c'_R = 5\,\text{kN/m}^3$

$W = 2.5\,\text{kN/m}^3$

$D = 0.1\,\text{kN/m}^2$

$h_v = 0.4\,\text{m}$

$T = 5\,\text{kN/m}$

$\theta = 45°$

$$F = \frac{(10+5) + [\{(18 - (9.8 \times 0.4)) + 2.5\} \times 0.6710 + (5 \times 0.7071)] \times 0.7002 + (5 \times 0.7071)}{[\{(18 + 2.5) \times 0.5736\} + 0.1] \times 0.8192}$$

$$F = \frac{15 + [\{((18 - 3.92) + 2.5) \times 0.6710\} + 3.5355] \times 0.7002 + 3.5355}{9.7147}$$

$$F = \frac{15 + 10.2654 + 3.5355}{9.7147}$$

$$F = \frac{28.8009}{9.7147}$$

$$F = 2.96$$

SENSITIVITY ANALYSIS

Increase in c'_R of 5 kN/m^3	increases F by 0.59
Increase in W of 2.5 kN/m^3	decreases F by 0.04
Increase in D of 0.1 kN/m^2	decreases F by 0.02
Increase in T of 5 kN/m	increases F by 0.71
Increase in h_w of 0.1 m	increases F by 0.08

REFERENCES

Al-Durrah, M.M. and Bradford, J.M. (1982) Parameters for describing soil detachment due to single waterdrop impact. *Soil Sci. Soc. Am. J.,* **46,** 836–40.

Appelmans, F., van Hove, J. and De Leenheer, L. (1980) Rain interception by wheat and sugar beet crops, in *Assessment of Erosion* (eds M.De Boodt and D.Gabriels). Wiley, Chichester, pp. 227–35.

Armstrong, C.L. and Mitchell, J.K. (1987) Transformations of rainfall by plant canopy. *Trans. Am. Soc. Agric. Engnrs.,* **30,** 688–96.

Babaji, G.A. (1987) Some plant stem properties and overland flow hydraulics. A laboratory simulation, PhD Thesis, Silsoe College, Cranfield Institute of Technology.

Bache, D.H. (1986) Momentum transfer to plant canopies: influence of structure and variable drag. *Atmospheric Environment,* **13,** 1681–7.

Bache, D.H. and MacAskill, I.A. (1984) *Vegetation in Civil and Landscape Engineering.* Granada Publishing, London.

Bagnold, R.A. (1941) *The Physics of Blown Sand and Desert Dunes.* Chapman and Hall, London.

Beasley, D.B., Huggins, L.F. and Monke, E.J. (1980) ANSWERS: a model for watershed planning. *Trans. Am. Soc. Agric. Engnrs.,* **23,** 938–44.

Biot, Y. (1990) THEPROM—An erosion productivity model, in *Soil Erosion on Agricultural Land* (eds J.Boardman, I.D.L.Foster and J.A.Dearing). Wiley, Chichester, pp. 465–79.

Bishop, D.M. and Stevens, M.E. (1964) Landslips on logged areas in southeast Alaska. *US Forest Service Research Paper NOR-1,* Northern Forest Experiment Station, Juneau, Alaska.

Boiffin, J. (1985) Stages and time-dependency of soil crusting in situ, in *Assessment of Soil Surface Sealing and Crusting* (eds F.Callebaut, D.Gabriels and M.De Boodt). Flanders Research Centre for Soil Erosion and Soil Conservation, Gent, pp. 91–8.

Brakensiek, D.L. and Rawls, W.J. (1983) Agricultural management effects on soil water processes. Part II. Green and Ampt parameters for crusting soils. *Trans. Am. Soc. Agric. Engnrs.,* **26,** 1753–7.

Brandt, C.J. (1989) The size distribution of throughfall drops under vegetation canopies. *Catena,* **16,** 507–24.

Brandt, C.J. (1990) Simulation of the size distribution and erosivity of raindrops and throughfall drops. *Earth Surf. Proc. Landf.,* **15,** 687–98.

Brown, C.B. and Sheu, M.S. (1975) Effects of deforestation on slopes. *J.Geotechnical Engineering Division, ASCE,* **101,** 147–65.

Bui, E.N. and Box, J.E. (1992) Stemflow, rain throughfall and erosion under canopies of corn and sorghum. *Soil Sci. Soc. Am. J.,* **56,** 242–7.

Carson, M.A. and Kirkby, M.J. (1972) *Hillslope Form and Process.* Cambridge University Press, Cambridge.

Carter, C.E., Greer, J.D., Braud, H.J. and Floyd, J.M. (1974) Raindrop characteristics in south central United States. *Trans. Am. Soc. Agric. Engnrs.,* **17,** 1033–7.

Chapman, G. (1948) Size of raindrops and their striking force at the soil surface in a red pine plantation. *Trans. Am. Geophys. Un.,* **29,** 664–70.

Cionco, R.M. (1965) A mathematical model for air flow in a vegetative canopy. *J. Appl. Met.,* **6,** 185–93.

Coppin, N.J. and Richards, I.G. (eds) (1990) *Use of Vegetation in Civil Engineering.* Construction Industry Research and Information Association/ Butterworths, London.

Coster, C. (1938) Surficial runoff and erosion on Java. *Tectona,* **31,** 613–728.

Cruse, R.M. and Larson, W.E. (1977) Effect of soil shear strength on soil detachment due to raindrop impact. *Soil Sci. Soc. Am. J.,* **41,** 777–81.

Denmead, O.T. (1976) Temperate cereals, in *Vegetation and the Atmosphere,* Vol. 2 (ed. J.L. Monteith). Academic Press, London, pp. 1–31.

De Ploey, J. (1981) The ambivalent effects of some factors of erosion. *Mem. Inst. Geol. Univ. Louvain,* **31,** 171–81.

De Ploey, J. (1982) A stemflow equation for grasses and similar vegetation. *Catena,* **9,** 139–52.

De Ploey, J. (1984) Hydraulics of runoff and loess loam deposition. *Earth Surf. Proc. Landf.,* **9,** 533–9.

De Ploey, J., Savat, J. and Moeyersons, J. (1976) The differential impact of some soil factors on flow, runoff creep and rainwash. *Earth Surf. Proc.,* **1,** 151–61.

Doorenbos, J. and Pruitt, W.O. (1977) Guidelines for predicting crop water requirements. *FAO Irrigation and Drainage Paper No. 24.*

Emama, E.L. (1988) Use of grass for control of hillside erosion. MSc Thesis, Silsoe College, Cranfield Institute of Technology.

Engelund, F. and Hansen, E. (1967) *A Monograph on Sediment Transport in Alluvial Streams.* Teknisk Forlag, København.

Engman, E.T. (1986) Roughness coefficients for routing surface runoff. *J. Irrigation and Drainage Division, ASCE.,* **112,** 39–53.

Farres, P. (1978) The role of time and aggregate size in the crusting process. *Earth Surf. Proc.,* **3,** 243–54.

Finney, H.J. (1984) The effect of crop covers on rainfall characteristics and splash detachment. *J. Agric. Engng. Res. ,* **29,** 337–43.

Foster, G.R. and Meyer, L.D. (1975) Mathematical simulation of upland erosion by fundamental erosion mechanics, in *Present and Prospective Technology for Predicting Sediment Yields and Sources.* USDA Agr. Res. Serv. Pub., ARS-S-40, pp.190–207.

Free, G.R. (1960) Erosion characteristics of rainfall. *Agric. Engng.,* **41,** 447–9, 455.

Govers, G. and Poesen, J. (1985) A field scale study of surface sealing on loam and sandy loam soils. Part I. Spatial variability of soil surface sealing and crusting, in *Assessment of Soil Surface Sealing and Crusting* (eds F.Callebaut, D.Gabriels and M.De Boodt). Flanders Research Centre for Soil Erosion and Conservation, Gent, pp. 171–82.

Govers, G. and Rauws, G. (1986) Transporting capacity of overland flow on a plane bed and on irregular beds. *Earth Surf. Proc. Landf.,* **11,** 515–24.

Gray, D.H. (1978) Role of woody vegetation in reinforcing soils and stabilising slopes. *Proceedings, Symposium on Soil Reinforcing and Stabilising Techniques in Engineering Practice.* NSW Institute of Technology, Sydney, Australia, pp. 253–306.

Gray, D.H. and Leiser, A.J. (1982) *Biotechnical Slope Protection and Erosion Control.* Van Nostrand Reinhold, New York.

Gray, D.H. and Megahan, W.F. (1981) Forest vegetation removal and slope stability in the Idaho batholith. *US Forest Research Paper INT-271.* Intermountain Forest and Range Experiment Station, Ogden, UT.

Greenway, D.R. (1987) Vegetation and slope stability, in *Slope Stability* (eds M.G.Anderson and K.S.Richards). Wiley, Chichester, pp. 187–230.

Grindley, J. (1969) The calculation of actual evaporation and soil moisture deficit over specified catchment areas. *Hydrological Memorandum No. 38,* Meteorological Office, Bracknell.

Hagen, L.J. and Lyles, L. (1988) Estimating small grain equivalents of shrub-dominated rangelands for wind erosion control. *Trans. Am. Soc. Agric. Engnrs.,* **31,** 769–75.

Hagen, L.J., Skidmore, E.L., Miller, P.L. and Kipp, J.E. (1981) Simulation of effect of wind barriers on airflow. *Trans. Am. Soc. Agric. Engnrs.,* **24,** 1002–8.

Hayes, J.C., Barfield, B.J. and Tollner, E.W. (1984) Performance of grass filters under laboratory and field conditions. *Trans. Am. Soc. Agric. Engnrs.,* **27,** 1321–31.

Herwitz, S.R. (1985) Interception storage capacities of tropical rainforest canopy trees. *J. Hydrology,* **77,** 237–52.

Herwitz, S.R. (1986) Infiltration-excess caused by stemflow in a cyclone-prone tropical rainforest. *Earth Surf. Proc. Landf.,* **11,** 401–12.

Herwitz, S.R. (1987) Raindrop impact and water flow on the vegetative surfaces of trees and the effects of stemflow and throughfall generation. *Earth Surf. Proc. Landf.,* **12,** 425–432.

Holtan, H.N. (1961) A concept for infiltration estimates in watershed engineering. *USD A Agric. Res. Serv. Pub., ARS-41–51.*

Hoogmoed, W.B. and Stroosnijder, L. (1984) Crust formation on sandy soils in the Sahel. I. Rainfall and infiltration. *Soil and Tillage Research,* **4,** 5–24.

Horton, R.E. (1919) Rainfall interception. *Monthly Weather Review,* **47,** 603–23.

Hsi, G. and Nath, J.H. (1970) Wind drag within a simulated forest. *J. Appl. Meteorology,* **9,** 592–602.

Hudson, N.W. (1963) Raindrop size distribution of high intensity storms. *Rhod. J. Agric. Res.,* **1,** 6–11.

Inoue, E. (1963) On the turbulent structure of air flow within crop canopies. *J. Met. Soc. Japan, Series 11,* **41,** 317–26.

Kowal, J.M. and Kassam, A.H. (1976) Energy load and instantaneous intensity of rainstorms at Samaru, northern Nigeria. *Trop. Agr. (Trinidad),* **53,** 185–97.

Laflen, J.M. (1987) Effect of tillage systems on concentrated flow erosion, in *Soil Conservation and Productivity* (ed. I.Pla Sentis). Sociedad Venezolana de la Ciencia del Suelo, Maracay, pp. 798–809.

Laflen, J.M. and Colvin, T.S. (1981) Effect of crop residue on soil loss from continuous row cropping. *Trans. Am. Soc. Agric. Engnrs.,* **24,** 605–9.

Landsberg, J.J. and James, G.B. (1971) Wind profiles in plant canopies: studies on an analytical model. *J. Appl. Ecol,* **8,** 729–41.

Leyton, L., Reynolds, E.R.C. and Thompson, F.B. (1967) Rainfall interception in forest and moorland, in *Forest Hydrology* (eds W.E.Sopper and H.W.Lull). Pergamon, Oxford, pp. 163–78.

Liddle, M.J. (1973) The effects of trampling and vehicles on natural vegetation. PhD Thesis, University College of North Wales, Bangor.

Maene, L.M. and Chong, S.P. (1979) Drop size distribution and erosivity of tropical rainstorms under the oil palm canopy. *Lapuran Penyelidikan Jabatan Sains Tanah 1977–78,* Universiti Pertanian Malaysia, Serdang, pp. 81–93.

Marshall, I.S. and Palmer, E.M. (1948) The distribution of raindrops with size. *J. Meteorology,* **5,** 165–6.

McKeague, J.A., Wang, C. and Coen, G.M. (1986) Describing and interpreting the macrostructure of mineral soils. *LRRI Contribution No. 84–50,* Agriculture Canada, Ottawa.

Merriam, R.A. (1973) Fog drip from artificial leaves in a fog wind tunnel. *Water Resources Research,* **9,** 1591–8.

Meyer, L.D. and Wischmeier, W.H. (1969) Mathematical simulation of the processes of soil erosion by water. *Trans. Am. Soc. Agric. Engnrs.,* **12,** 754–8, 762.

Monteith, J.L. (1973) *Principles of Environmental Physics.* Edward Arnold, London.

Morgan, R.P.C. (1980) Field studies of sediment transport by overland flow. *Earth Surf. Proc.,* **5,** 307–16.

Morgan, R.P.C. (1985) Effect of corn and soybean canopy on soil detachment by rainfall. *Trans. Am. Soc. Agric. Engnrs.,* **28,** 1135–40.

Morgan, R.P.C. (1989) Design of in-field shelter systems for wind erosion control, in *Soil Erosion Protection Measures in Europe* (eds U.Schwertmann, R.J.Rickson and K.Auerswald), Soil Technology Series No. 1, Catena Publications, Cremlingen-Destedt, pp. 15–23.

Morgan, R.P.C. and Finney, H.J. (1987) Drag coeffficients of single crop rows and their implications for wind erosion control, in *International Geomorphology 1986.* Part II (ed. V.Gardiner). Wiley, Chichester, pp. 449–58.

Morgan, R.P.C., Finney, H.J. and Williams, J.S. (1986) Fundamental plant parameters for wind erosion control. Final Report to the UK Agriculture and Food Research Council, Research Grant No. AG63/170.

Morgan, R.P.C., Finney, H.J. and Williams, J.S. (1988) Leaf properties affecting crop drag coefficients: implications for wind erosion control, in *Land Conservation for Future Generations* (ed. S.Rimwanich). Department of Land Development, Ministry of Agriculture and Cooperatives, Bangkok, pp. 885–93.

Morin, J., Benyamini, Y. and Michaeli, A. (1981) The effect of raindrop impact on the dynamics of soil surface crusting and water movement in the profile. *J. Hydrology,* **52,** 321–6.

Mosley, M.P. (1982) The effect of a New Zealand beech forest canopy on the kinetic energy of water drops and on surface erosion. *Earth Surf. Proc. Landf.,* **7,** 103–7.

Moss, A.J. and Green, T.W. (1987) Erosive effects of the large water drops (gravity drops) that fall from plants. *Austral. J. Soil Res.,* **25,** 9–20.

Nielsen, S.A. and Styczen, M. (1986) Development of an areally distributed soil erosion model , in *Partikulaert bundet stoftransport i vand og jorderosjon* (ed. B.Hasholt). Nordisk Hydrologisk Program Rapport No. 14, pp. 293–302.

Noble, C.A. (1981) The effect of plant cover on the erosivity of rainfall. MSc Thesis, Silsoe College, Cranfield Institute of Technology.

Noble, C.A. and Morgan, R.P.C. (1983) Rainfall interception and splash detachment with a Brussels sprouts plant: a laboratory simulation. *Earth Surf. Proc. Landf.,* **8,** 569–77.

O'Loughlin, C.L. (1984) Effectiveness of introduced forest vegetation for protecting against landslides and erosion in New Zealand's steeplands. Paper presented to Symposium on effects of forest land use on erosion and slope stability, Honolulu, Hawaii.

Park, S.W. (1981) Modeling soil erosion and sedimentation on small agricultural watersheds. PhD Thesis, University of Illinois.

Park, S.W., Mitchell, J.K. and Scarborough, J.N. (1982) Soil erosion simulation on small watersheds: a modified ANSWERS model. *Trans. Am. Soc. Agric. Engnrs.,* **25,** 1581–8.

Penman, H.L. (1949) The dependence of transpiration on weather and soil conditions. *J. Soil Sci.,* **1,** 74–89.

Quansah, C. (1985) Rate of soil detachment by overland flow, with and without rain, and its relationship with discharge, slope steepness and soil type, in *Soil Erosion and Conservation* (eds S.A.El Swaify, W.C.Moldenhauer and A.Lo) Soil Conservation Society of America, Ankeny, IA, pp. 406–23.

Quinn, N.W., Morgan, R.P.C. and Smith, A.J. (1980) Simulation of soil erosion by human trampling. *J. Environmental Management,* **10,** 155–65.

Randall, J.M. (1969) Wind profiles in an orchard plantation. *Agric. Meteorol,* **6,** 439–52.

Rauws, G. and Covers, G. (1988) Hydraulic and soil mechanical aspects of rill generation on agricultural soils. *J. Soil Sci.,* **39,** 111–24.

Rawls, W.J., Brakensiek, D.L. and Soni, B. (1983) Agricultural management effects on soil water processes. Part I. Soil water retention and Green and Ampt infiltration parameters. *Trans. Am. Soc. Agric. Engnrs.,* **26,** 1747–52.

Ree, W.O. (1949) Hydraulic characteristics of vegetation for vegetated waterways. *Agric. Engng.,* **30,** 184–7, 189.

Rose, C.W., Williams, I.R., Sander, G.C. and Barry, D.A. (1983) A mathematical model of soil erosion and deposition processes. I. Theory for a plane element. *Soil Sci. Soc. Am. J.,* **47,** 991–5.

Rutter, A.J. and Morton, A.J. (1977) A predictive model of rainfall interception in forests. III. Sensitivity of the model to stand parameters and meteorological variables. *J. Appl. Ecol.,* **14,** 567–88.

Schoklitsch, A. (1950) *Handbuch des Wassbaues.* Springer, Wien.

Seginer, I. (1972) Windbreak drag calculated from the horizontal velocity field. *Boundary Layer Meteorology,* **3,** 87–97.

Shaw, R.H. and Pereira, A.R. (1982) Aerodynamic roughness of a plant canopy: a numerical experiment. *Agric. Met.,* **26,** 51–65.

Singer, M.J. and Blackard, J. (1978) Effect of mulching on sediment in runoff from simulated rainfall. *Soil Sci. Soc. Am. J.,* **42,** 481–6.

Skidmore, E.L. and Hagen, L.J. (1977) Reducing wind erosion with barriers. *Trans. Am. Soc. Agric. Engnrs.,* **20,** 911–15.

Styczen, M. and Høgh-Schmidt, K. (1986) A new description of the relation between drop sizes, vegetation and splash erosion, in *Partikulaert bundet stoftransport i vand og jorderosjon* (ed. B. Hasholt). Nordisk Hydrologisk Program Rapport No. 14, pp. 255–71.

Styczen, M. and Høgh-Schmidt, K. (1988) A new description of splash erosion in relation to raindrop size and vegetation, in *Erosion Assessment and Modelling* (eds R.P.C.Morgan and R.J. Rickson). Commission of the European Communities Report No. EUR 10860 EN, pp. 147–98.

Styczen, M. and Nielsen, S.A. (1989) A view of soil erosion theory, process-research and model building: possible interactions and future developments. *Quaderni di Scienza del Suolo,* **2,** 27–45.

Temple, D.M. (1982) Flow retardance of submerged grass channel linings. *Trans. Am. Soc. Agric. Engnrs.,* **25,** 1300–3.

Tengbeh, G.T. (1989) The effect of grass cover on bank erosion. PhD Thesis, Silsoe College, Cranfield Institute of Technology.

Thom, A.S. (1971) Momentum absorption by vegetation . *Quart. J. Roy. Met. Soc.,* **97,** 414–28.

Thom, A.S. (1975) Momentum, mass and heat exchange of plant communities, in *Vegetation and the Atmosphere,* Vol. 1 (ed. J.L.Monteith). Academic Press, London, pp. 57–109.

Thornes, J.B. (1988a) Competitive vegetation-erosion model for Mediterranean conditions, in *Erosion Assessment and Modelling* (eds R.P.C. Morgan and R.J.Rickson). Commission of the European Communities Report No. EUR 10860 EN, pp. 255–82.

Thornes, J.B. (1988b) Erosional equilibria under grazing, in *Conceptual Issues in Environmental Archaeology* (eds J.Bintliff, D.Davidson and E.Grant). Edinburgh University Press, Edinburgh, pp.193–210.

Thornes, J.B. (1990) The interaction of erosional and vegetational dynamics in land degradation: spatial outcomes, in *Vegetation and Erosion* (ed. J.B. Thornes). Wiley, Chichester, pp. 41–53.

Tollner, E.W., Barfield, B.J. and Hayes, J.C. (1982) Sedimentology of erect vegetal filters. *J. Hydraulics Division, ASCE,* **108,** 1518–31.

Torri, D., Sfalanga, M. and Del Sette, M. (1987) Splash detachment, runoff depth and soil cohesion. *Catena,* **14,** 149–55.

Tsukamoto, Y. and Kusakabe, O. (1984) Vegetative influences on debris slide occurrences on steep slopes in Japan. Paper presented to Symposium on Effects of forest land use on erosion and slope stability, Honolulu, Hawaii.

US Soil Conservation Service (1954) *Handbook of Channel Design for Soil and Water Conservation.* USDA Tech. Pub., SCS-TP-61.

Valentin, C. (1985) Effects of grazing and trampling on soil deterioration around recently drilled water holes in the Sahelian zone, in *Soil Erosion and Conservation* (S.A.El-Swaify, W.C.Moldenhauer and A.Lo). Soil Conservation Society of America, Ankeny, IA, pp. 51–65.

Van Elewijck, L. (1988) Influence of leaf and branch slope on stemflow amount. Paper presented to British Geomorphological Research Group Symposium on Vegetation and geomorphology, Bristol, UK.

Van Elewijck, L. (1989) Stemflow on maize: a stem-flow equation and the influence of rainfall intensity on stemflow amount, *Soil Technology,* **2,** 41–8.

Voetberg, K.S. (1970) *Erosion on Agricultural Lands.* Agricultural University, Wageningen.

Waldron, L.J. (1977) The shear resistance of root-permeated homogeneous and stratified soil. *Soil Sci. Soc. Am. J.,* **41,** 343–9.

Waldron, L.J. and Dakessian, S. (1981) Soil reinforcement by roots: calculation of increased soil shear resistance from root properties. *Soil Sci.,* **132,** 427–35.

Wang, W.L. and Yen, B.C. (1974) Soil arching in slopes. *J. Geotechnical Engineering Division, ASCE,* **100,** 61–78.

Wiersum, K. (1985) Effects of various vegetation layers of an *Acacia auriculiformis* forest plantation on surface erosion in Java, Indonesia, in *Soil Erosion and Conservation* (eds S.A.El-Swaify, W.C.Moldenhauer and A.Lo). Soil Conservation Society of American, Ankeny, IA, pp. 79–89.

Wiersum, K., Budirijanto, P. and Rhomdoni, D. (1979) Influence of forests on erosion. Seminar on the erosion problem in the Jatiluhur area. Institute of Ecology, Padjadjaran University, Bandung, Report No. 3.

Wischmeier, W.H. (1975) Estimating the soil loss equation's cover and management factor for undisturbed areas, in *Present and Prospective Technology for Predicting Sediment Yields and Sources.* USDA Agr. Res. Serv., Pub., ARS-S-40, pp. 118–24.

Wischmeier, W.H. and Smith, D.D. (1978) Predicting rainfall erosion losses. *USDA Agr. Res. Serv. Handbook 537.*

Withers, B. and Vipond, S. (1974) *Irrigation: Design and Practice.* Batsford, London.

Wossenu Abtew, Gregory, J.M. and Borrelli, J. (1989) Wind profile: estimation of displacement height and aerodynamic roughness. *Trans. Am. Soc. Agric. Engnrs.,* **32,** 521–7.

Wright, J.L. and Brown, K.W. (1967) Comparison of momentum and energy balance methods of computing vertical transfer within a crop. *Agron. J.,* **59,** 427–32.

Yen, C.P. (1972) Study on the root system form and distribution habit of the ligneous plants for soil conservation in Taiwan (preliminary report). *J. Chinese Soil & Water Conserv.,* **3,** 179–204.

Yen, C.P. (1987) Tree root patterns and erosion control, in *Proceedings of the International Workshop on Soil Erosion and Its Countermeasures* (ed. S.Jantawat). Soil and Water Conservation Society of Thailand, Bangkok, pp. 92–111.

Ziemer, R.R. (1981) Roots and stability of forested slopes. *Int. Assoc. Hydrol. Sci., Pub. No. 132,* pp. 343–61.

Zinke, P.J. (1967) Forest interception studies in the US, in *Forest Hydrology* (eds W.E.Sopper and H.W.Lull). Pergamon, Oxford, pp. 137–61.